JCB Article

The organization of engaged and quiescent translocons in the endoplasmic reticulum of mammalian cells

Erik L. Snapp, Gretchen A. Reinhart, Brigitte A. Bogert, Jennifer Lippincott-Schwartz, and Ramanujan S. Hegde

Cell Biology and Metabolism Branch, National Institute of Child Health and Human Development, National Institutes of Health, Bethesda, MD 20892

Protein translocons of the mammalian endoplasmic reticulum are composed of numerous functional components whose organization during different stages of the transport cycle in vivo remains poorly understood. We have developed generally applicable methods based on fluorescence resonance energy transfer (FRET) to probe the relative proximities of endogenously expressed translocon components in cells. Examination of substrate-engaged translocons revealed oligomeric assemblies of the Sec61 complex that were associated to varying degrees with other essential components including the signal recognition particle receptor, TRAM and the TRAP complex. Remarkably, these components not only remained assembled but also had a similar, yet distinguishable, organization both during and after nascent chain translocation. The persistence of preassembled and complete translocons between successive rounds of transport may facilitate highly efficient translocation in vivo despite temporal constraints imposed by ongoing translation and a crowded cellular environment.

Introduction

The biogenesis of secretory and membrane proteins in mammalian cells involves several discrete steps that include targeting of nascent polypeptides to the ER, their cotranslational transport across or integration into the ER membrane, and various modification, folding, and maturation events (for review see Rapoport et al., 1996; Johnson and van Waes, 1999). The ability to reconstitute this entire process in a cell-free system amenable to biochemical fractionation has allowed each stage to be studied in isolation and has facilitated the identification of the respective factors involved. Collectively, the multiple components that define the machinery for cotranslational protein translocation constitute the translocon.

Central among the translocon components is the heterotrimeric Sec61 complex (composed of α, β, and γ subunits), multiple copies of which are thought to be assembled to form the core of a protein-conducting translocation channel (Hanein et al., 1996; Beckmann et al., 1997, 2001; Menetret et al., 2000; Morgan et al., 2002). Signal sequence–containing nascent polypeptides, recognized first by the cytoplasmic signal recognition particle (SRP), are targeted to the Sec61 channel by another translocon component, the heterodimeric SRP receptor (SR; for review see Rapoport et al., 1996). Although some nascent chains can subsequently insert directly into the Sec61 channel (Jungnickel and Rapoport, 1995), most substrates require the aid of at least one of two additional translocon components, the TRAM protein (Gorlich and Rapoport, 1993; Voigt et al., 1996) and/or the heterotetrameric TRAP complex (Fons et al., 2003). Once these critical first steps result in a commitment to initiate substrate translocation, other translocon components can interact with the nascent chain during its transport to catalyze reactions such as signal sequence cleavage and glycosylation. Thus, a biochemical approach has provided the general framework for ordering a succession of individual steps whose mechanistic basis can be further dissected.

In spite of this level of mechanistic insight, basic aspects of translocon composition and organization during its functional cycle in vivo remain poorly or not at all understood. One of the most elemental yet unresolved issues in this regard is the fate of a translocon, and in particular the translocation channel, between rounds of substrate transport. The first of two general possibilities is that the constituents of the channel, whose assembly would be directed by a nascent

The online version of this article includes supplemental material.

Address correspondence to R.S. Hegde, Cell Biology and Metabolism Branch, National Institute of Child Health and Human Development, National Institutes of Health, 18 Library Dr., Bldg. 18, Rm. 101, Bethesda, MD 20892. Tel.: (301) 496-4855. Fax: (301) 402-0078. email: hegder@mail.nih.gov

Key words: FRET; TRAP; protein translocation; Sec61; TRAM

Abbreviations used in this paper: CNX, calnexin; FRET, fluorescence resonance energy transfer; SR, SRP receptor; SRP, signal recognition particle.

substrate, are disassembled upon completion of transport. Alternatively, the channel may remain assembled when not in use and closed on one or both ends to prevent compromising the permeability barrier of the ER.

The currently available data from biochemical studies have yielded evidence for both situations. Despite the lack of copurification of various components of the translocon, they can nonetheless be coreconstituted into proteoliposomes that support functional protein transport (Gorlich and Rapoport, 1993). In addition, purified Sec61 complex incorporated into lipid vesicles was not observed to oligomerize into channel-like structures until the addition of ribosomes (Hanein et al., 1996). Both of these observations show that translocation channels can be assembled de novo from their isolated constituents, lending credence to a model involving use-dependent assembly and disassembly of the translocon.

In contrast, vacating the translocation channel of its nascent chain in vitro with puromycin did not result in a gross structural change or a reduction in the number of translocons that were observed by freeze-fracture EM (Hanein et al., 1996). In addition, puromycin was observed to stimulate the flux of both ions (Simon and Blobel, 1991) and a noncharged small molecule (Roy and Wonderlin, 2003) through channels that had presumably been occluded by translocating substrates. Thus, translocons may not disassemble or even close upon completion of substrate transport.

However, it is presumed that a pore large enough to transport a protein could not remain open while not in use because the permeability barrier of the ER would be compromised (Crowley et al., 1994). Indeed, ER-derived microsomal vesicles after removal of their lumenal contents with alkaline extraction were permeable to ions through channels that could be sterically blocked with either ribosomes or antibodies against Sec61α or TRAM (Hamman et al., 1998). These channels, speculated to reflect the configuration of translocons between rounds of translocation, were not only smaller than an active translocon (pore size of ~0.9–1.7 nm vs. ~4–6 nm) but also capable of being sealed to ions by the ER lumenal chaperone BiP (Hamman et al., 1998). These observations suggest a model in which completion of translocation results in a substantial change in the organization of translocons that remain assembled between rounds of transport. However, such large changes in pore size have yet to be observed in cryo-EM images (at ~1.5–2 nm resolution) comparing translocons assembled onto either empty or nascent chain–containing ribosomes (Menetret et al., 2000; Beckmann et al., 2001). Recently, an X-ray structure of the archaeal Sec61 homologue (termed SecYEβ) suggested a reversibly occludable pore within a single heterotrimer (Van den Berg et al., 2004), raising the possibility that the functional state of a translocon may change without necessarily requiring changes in the overall assembly or organization of translocon components. Thus, the nature of organizational changes during the transport cycle of the core Sec61 translocation channel remains uncertain, with different conclusions being reached with different methods.

Although considerable functional data are available for SR and to a lesser extent TRAM and the TRAP complex, little is known regarding the contributions of these components to either the composition or the architecture of a native translocon. The functional activities of each protein appear to be required at specified times during substrate translocation. Whether or not these proteins are stably assembled into native translocons or recruited transiently in a use-dependent manner is not known. Analysis by blue native PAGE did not reveal clear evidence for oligomeric complexes containing any two of the essential translocon components Sec61, SR, TRAM, or TRAP (Wang and Dobberstein, 1999). Similarly, no two of these components have been observed to copurify in studies of their functional purification and reconstitution (Gorlich et al., 1992; Gorlich and Rapoport, 1993; Fons et al., 2003). Thus, biochemical analyses to this point have failed to clearly reveal stable interactions between various translocon components that must nonetheless be near each other, at least transiently, during specific stages of translocation.

Together, these various observations show that not only is the issue of translocation channel assembly and disassembly uncertain but also the nature of different structural states representing active and inactive translocons remains obscure. To begin addressing these unanswered questions regarding translocon organization, we have developed a method based on fluorescence resonance energy transfer (FRET) to probe the relative proximities of endogenously expressed translocon components in cells at low nanometer resolution. This approach was subsequently exploited to provide new insights into both the composition and organizational state of the translocon during its functional cycle in cells.

Results

Experimental rationale and strategy

An investigation of translocon composition and organization in cells requires methodology capable of providing information on the relative proximities of the constituent proteins at low nanometer resolution. With such a tool, an analysis of the positions of different combinations of translocon components can be used to infer their direct associations, and hence general features of their overall organization. By examining changes in this organization under different cellular conditions, one can potentially gain insight into the critical transition between inactive and active functional states of translocons. In this manner, we sought to distinguish between different viable models of translocon dynamics based on in vitro studies.

FRET between two fluorescently labeled proteins provides a highly sensitive and specific probe of their proximity in the low- to subnanometer range (see online supplemental material and references therein, available at http://www.jcb.org/cgi/content/full/jcb.200312079/DC1). To apply this methodology to the endogenously expressed native translocons of cultured cells, we decided to label individual components using epitope-specific antibodies directly conjugated to fluorescent dyes. We reasoned that despite their large size, FRET between labeled antibodies could potentially provide useful information regarding the proximities and organization of their bound antigens. In the first part of this work (presented largely in online supplemental material), we combined modeling and simulations to consider the feasibility of this approach to address the anticipated questions. This

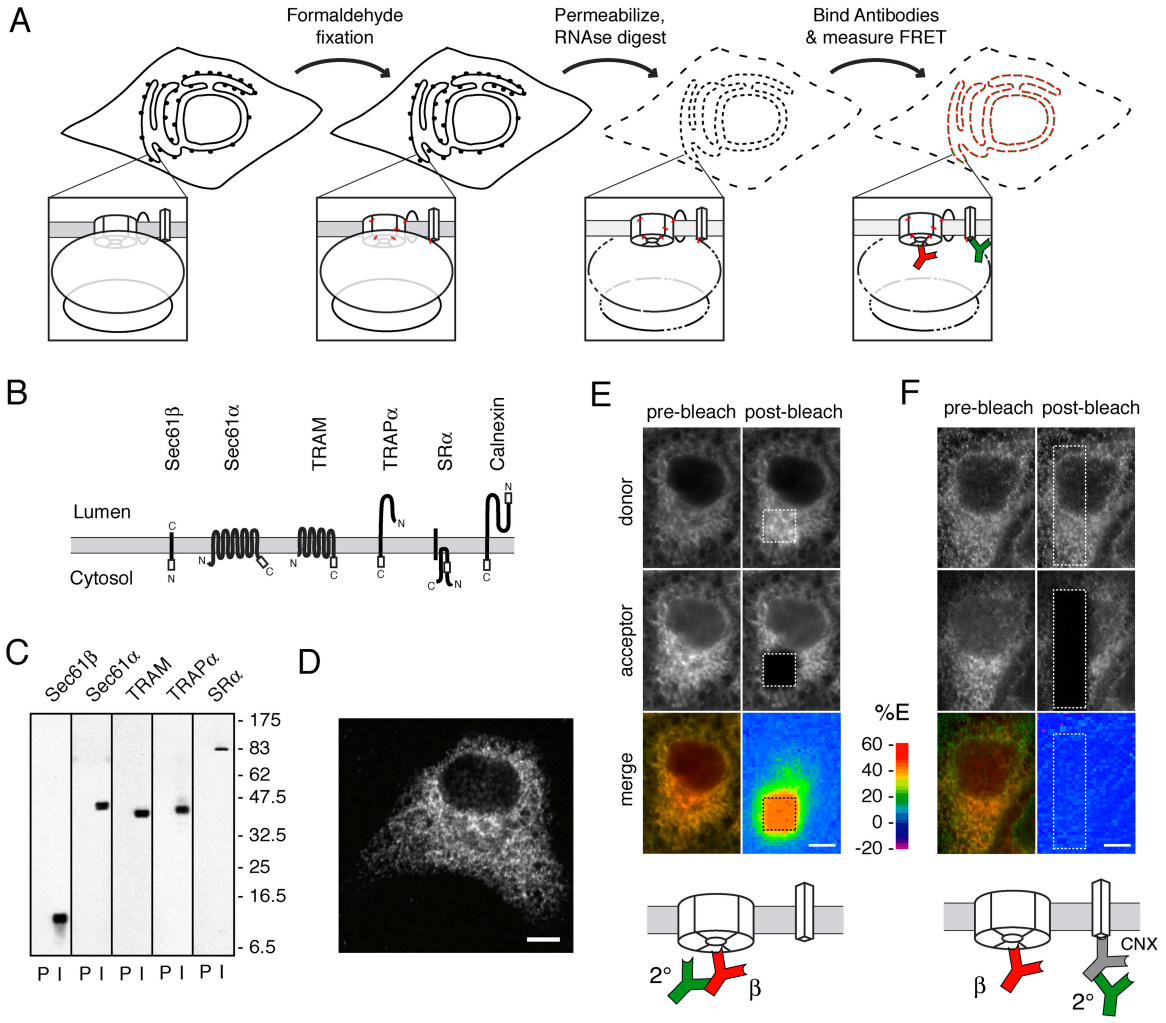

Figure 1. **Detection of FRET between fluorescently conjugated antibodies in situ.** (A) Scheme for preparation of cells for FRET analysis. Insets show an individual ribosome–translocon complex. Red hatches in the inset indicate formaldehyde cross-links between interacting proteins. The dotted lines indicate permeabilization (of the cellular membranes) or partial digestion (in the case of the ribosome). In this and all subsequent diagrams, the Cy3-labeled donor and Cy5-labeled acceptor antibodies are green and red, respectively. See text for complete details. (B) Topology maps of ER proteins analyzed in this study. The positions of peptide epitopes for antibodies are indicated with white boxes. (C) Western blot analysis of canine pancreatic ER microsomes with preimmune (P) or immune (I) antisera against the indicated antigens. (D) Indirect immunofluorescence microscopy of MDCK cells with anti-Sec61β. (E) MDCK cells were stained with Sec61β_{Cy5} followed by 2°$_{Cy3}$. Shown are the fluorescence images for Cy3 (donor), Cy5 (acceptor), and merged channels (prebleach images). The Cy5 dye in the region indicated by the box was selectively photobleached, and the donor and acceptor channels imaged a second time (postbleach images). The percent change in donor intensity between the pre- and postbleach images was calculated and represented as a pseudocolor map. Note the >40% increase in donor fluorescence intensity within the boxed area upon acceptor photobleaching. (F) MDCK cells were stained with 2°$_{Cy3}$ bound to unlabeled anti-CNX followed by Sec61β_{Cy5}, and the images were collected and analyzed as in E. Note the near absence of change in donor intensity upon acceptor photobleaching. The color scale represents the percentage of energy transfer (%E) in the pseudocolored map. Bars: (D–F) 5 μm.

methodology was applied to address unanswered questions regarding the composition and organization of translocons at different stages of the transport cycle in cells.

Modeling and simulations of FRET between dye-conjugated antibodies bound to antigens in various configurations and densities were used to estimate the resolving power of antibody-mediated FRET (see online supplemental material). From these analyses, we conclude that antibody-mediated FRET should be capable of the following activities: (a) distinguishing differences in antigen proximity at the 0.5–1-nm scale; (b) distinguishing between assembled and unassembled states of oligomeric structures; and (c) discriminating even small differences in relative distances that might accompany a structural change of a multiprotein complex. These conclusions suggested that, in principle, the organization of multiprotein complexes could be assessed with antibody probes. Thus, if endogenous translocon components could be labeled with dye-conjugated antibodies while maintaining their overall organization, FRET between the dyes should provide insight into translocon composition and organization.

To apply these ideas, we used variations of previous methodology to label cellular proteins while preserving their relative proximities (Fig. 1 A). Intact live cells are rapidly fixed in formaldehyde to stabilize the in situ organization of cellu-

lar proteins with covalent cross-links between closely juxtaposed components. Because cross-links mediated by formaldehyde are extremely short (~0.2 nm) and rapidly induced, proteins are effectively immobilized in place without an opportunity to substantially change their relative proximities or organization (Jackson, 1999). Because the preservation is covalent and, under the conditions applied here, effectively irreversible, the samples can subsequently be subjected to nonphysiological conditions that would have otherwise disrupted labile or transient interactions.

This condition allows the fixed cells to be permeabilized and labeled with fluorescent antibodies without changing the organization of the translocon components or the multiprotein complexes in which they are assembled (Fig. 1 A). Due to the fixed nature of the antigens, the bivalent antibodies cannot induce gross changes in the existing organization of their antigens. Instead, the antibodies serve to "mark" the positions of their antigens with fluorescent probes whose relative proximities can subsequently be assessed by FRET (e.g., as modeled in online supplemental material). Thus, the ability to assess what the state of the translocon had been in intact cells under different conditions should permit us to ask if, in cells, translocon organization changes at different stages of the translocation cycle.

The sensitivity and specificity of FRET between dye-conjugated antibodies

Antibodies raised against small peptide epitopes in the cytoplasmic domains of the translocon components Sec61α, Sec61β, TRAM, TRAPα, and SRα (Fig. 1 B) were characterized by immunoblotting against ER-derived microsomes and cell lysates and indirect immunofluorescence of cultured cells (Fig. 1, C and D; and Fig. S1 A, available at http://www.jcb.org/cgi/content/full/jcb.200312079/DC1; unpublished data). Importantly, maximal antibody binding to certain epitopes required pretreatment of the fixed and permeabilized cells with RNase (see online supplemental material; Fig. S1, B and C). Although RNase may not significantly disrupt overall ribosome structure, particularly in fixed samples, it would still digest surface-exposed loops of rRNA. The removal of these loops, together with the fact that even undigested ribosomes appear to be separated from translocons by a substantial gap (Hanein et al., 1996; Beckmann et al., 1997, 2001; Menetret et al., 2000; Morgan et al., 2002), appears to be sufficient to provide antibody access to translocon component epitopes that are otherwise sterically occluded. Whatever the precise explanation, the unmasking of epitopes is an important step that facilitates a uniform level of labeling in cells regardless of whether their translocons were actively engaged by translating ribosomes or not (Fig. S1, E and F). Therefore, we included this RNase-mediated unmasking step in all of the experiments.

For FRET analyses, antibodies were conjugated to the fluorescent dyes Cy3 or Cy5, which serve as the donor and acceptor, respectively (see online supplemental material). Then, we established conditions that allow the detection of FRET between closely juxtaposed but not more widely separated labeled antibodies. In this experiment, Cy5-conjugated anti-Sec61β ($Sec61\beta_{Cy5}$) bound to its antigen in MDCK cells served as the acceptor. The donor antibody, a Cy3-conjugated anti–rabbit secondary antibody (2°_{Cy3}), was positioned in one of two places (Fig. 1, E and F, diagrams). In Fig. 1 E, the 2°_{Cy3} was bound directly to the $Sec61\beta_{Cy5}$ antibody, ensuring that all donor antibodies are adjacent to an acceptor. Alternatively, the 2°_{Cy3} antibody was bound to an unlabeled antibody against the COOH terminus of calnexin (CNX; Fig. 1 F), a resident ER membrane protein involved in the posttranslational quality control of proteins (Bergeron et al., 1994). Because in either case both the acceptor and donor antibodies are bound (either directly or indirectly) to ER antigens, their fluorescent signals colocalize at the resolution of light microscopy (Fig. 1, E and F). In striking contrast, the different relative positions of the donor could be readily discriminated by assessing the FRET between the Cy3 and Cy5 dyes (Fig. 1, E and F).

To quantitatively reveal and measure FRET, the Cy3 donor fluorescence is monitored before and after the Cy5 acceptor dyes are selectively destroyed by high-intensity laser photobleaching. Upon destruction of Cy5, the Cy3 fluorescence should increase by an amount corresponding to the proportion of energy that had been transferred to Cy5 (Kenworthy, 2001). It should be noted that in addition to FRET, the apparent increase in Cy3 fluorescence intensity can, under some circumstances, be caused by the photoconversion of Cy5 to a different fluorescent species that partially overlaps with the Cy3 spectra. However, in our work, this possibility was not found to be a significant source of error in the Cy3 measurements (see online supplemental material for a detailed discussion). Thus, the increase in Cy3 intensity seen with Cy5 photobleaching is largely reflective of FRET between the two fluorophores.

This increase in fluorescence intensity can be qualitatively appreciated by comparing the pre- and postbleach images of the donor (Fig. 1 E). The extent of donor dequenching can be measured in each 8×8 pixel region (equal to $\sim 0.3\ \mu m^2$) and represented as a pseudocolored map that quantitatively displays the percentage of energy transfer within the photobleached region. A comparison of the percentage of energy transfer maps for Fig. 1 (E and F) reveals that the overall efficiency of FRET from the 2°_{Cy3} to $Sec61\beta_{Cy5}$ can vary from $>40\%$ (Fig. 1 E) to $<2\%$ (Fig. 1 F) depending on whether or not the two antibodies are directly juxtaposed or simply in the same subcellular compartment. Thus, sublight resolution differences in the relative positions of donor- and acceptor-labeled antibodies can readily be distinguished and quantified by FRET measured with acceptor photobleaching methodology.

Detection of protein proximities within translocons

Distinguishing between different models of translocon dynamics requires the reliable discrimination of assembled from disassembled multiprotein structures. To determine if antibody-mediated FRET can provide this resolution, we assessed the proximities between two resident ER membrane proteins that should be largely assembled versus two that are primarily disassociated at steady state. For the assembled case, we chose Sec61α and Sec61β, constituents of a stable Sec61 complex whose subunits do not appear to exist in a significant free pool (Gorlich and Rapoport, 1993). For comparison, we probed FRET between Sec61β and another

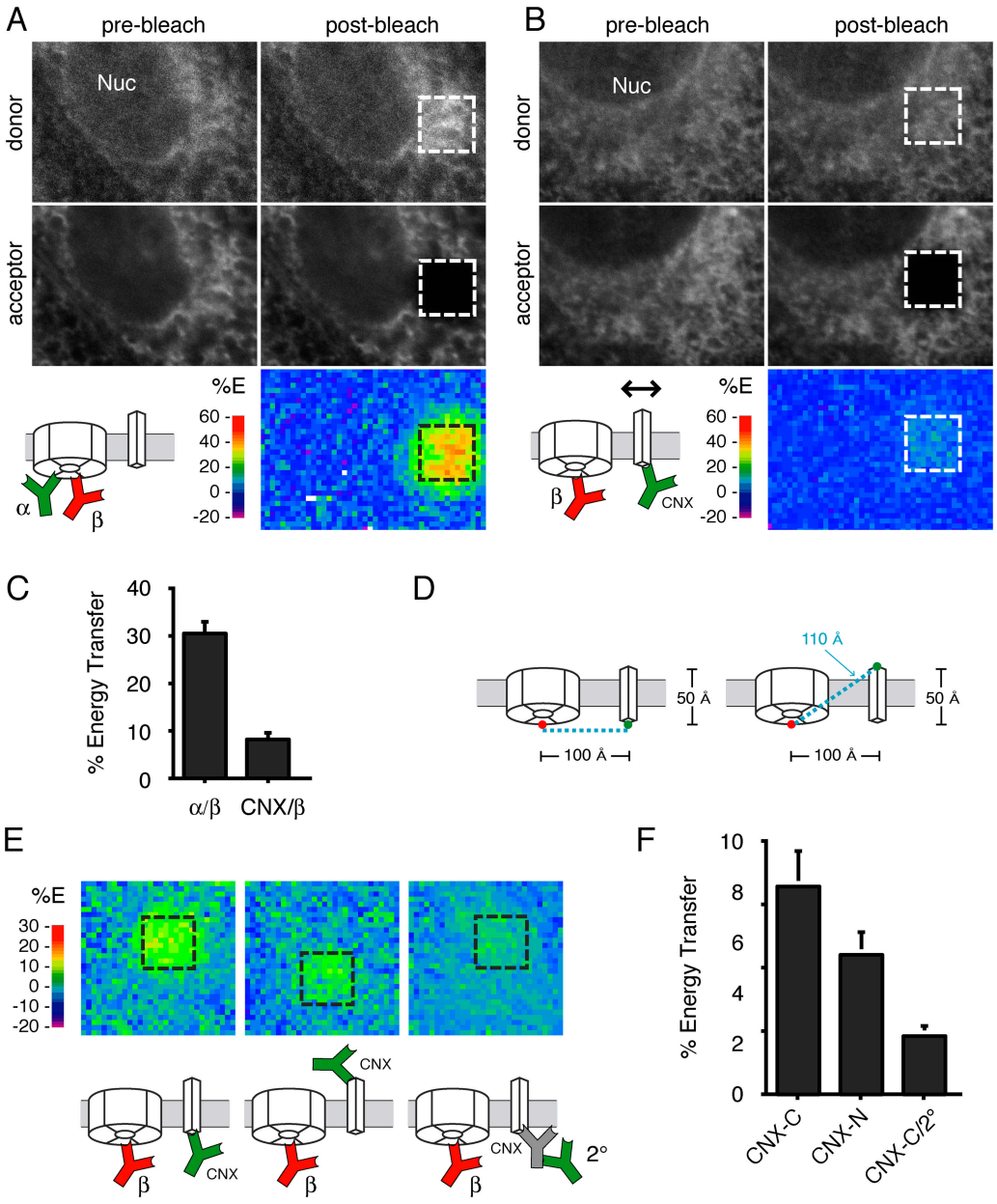

Figure 2. **Discrimination of protein proximities with low nanometer resolution.** (A and B) MDCK cells were double labeled with Sec61α_{Cy3} and Sec61β_{Cy5} (A) or CNX$_{Cy3}$ and Sec61β_{Cy5} (B) and analyzed for FRET as in Fig. 1 E. (C) Quantitative analysis of FRET between the antibody configurations shown in A and B. The antibody pair is indicated on the x-axis, with Sec61β_{Cy5} serving as the acceptor in each case. Each bar represents the mean ± SD ($n = 10$), with statistically significant differences ($P < 0.01$ using t test) being observed between the two conditions. (D) Illustration of the relative difference in distance for antibodies on the cytoplasmic and lumenal sides of CNX. Note that moving the donor antibody to the other side of an ~5-nm-thick membrane changes the distance to the acceptor antibody by only ~1 nm in this example. (E) Representative energy transfer maps of FRET to Sec61β_{Cy5} from Cy3-labeled antibodies in three different positions. The left and middle panels used directly conjugated anti-CNX antibodies against the COOH and NH_2 terminus, respectively. The right panel used 2°$_{Cy3}$ bound to an unlabeled anti-CNX COOH terminus antibody. The color scale is different than in A and B to enhance visualization of differences between the energy transfer maps. (F) Quantitative analysis of FRET between the antibody configurations shown in E. The donor antibody is indicated on the x-axis, while Sec61β_{Cy5} served as the acceptor in each case. Each bar represents the mean ± SD ($n = 10$), with statistically significant differences ($P < 0.01$ using t test) being observed between any two conditions.

resident ER membrane protein expressed at similar levels, CNX. Although CNX is not generally considered a core component of the translocon, a small population of CNX has been demonstrated to interact with a subset of proteins still undergoing translocation (Molinari and Helenius, 2000). Thus, the transient nature of the interactions between CNX and nascent translocating proteins results in the close proximity between Sec61β and CNX for only a small percentage of the total CNX, thereby representing a largely unassembled state between these two ER proteins.

FRET, comparable to that seen for directly interacting donor and acceptor antibodies, was observed between Sec61α_{Cy3} and Sec61β_{Cy5} (Fig. 2, A and C). For the same Sec61β_{Cy5} acceptor, a CNX$_{Cy3}$ donor antibody directed

against the cytoplasmic COOH terminus of CNX exhibited severalfold lower FRET efficiency compared with Sec61α_{Cy3} (Fig. 2, B and C). In addition to the markedly lower FRET for the CNX$_{Cy3}$ donor, several other observations confirmed the specificity of the Sec61α_{Cy3}/Sec61β_{Cy5} FRET. First, omission of the Sec61β_{Cy5} resulted in no observable FRET (i.e., no change in Sec61α_{Cy3} intensity on photobleaching in the Cy5 channel; unpublished data). Second, inclusion of a competitor Sec61β peptide resulted in reduced labeling by Sec61β_{Cy5} and correspondingly lower FRET (unpublished data). Third, reducing the concentration of Sec61β_{Cy5} also resulted in lower FRET (Fig. S9, available at http://www.jcb.org/cgi/content/full/jcb.200312079/DC1), as would be expected for lower occupancy levels of acceptor antigens with antibody (Fig. S4 E, available at http://www.jcb.org/cgi/content/full/jcb.200312079/DC1). In contrast, changing the levels of Sec61α_{Cy3}, although changing the overall brightness of the donor labeling, did not affect FRET efficiency significantly (Fig. S8, available at http://www.jcb.org/cgi/content/full/jcb.200312079/DC1), also as predicted from theoretical considerations (Fig. S4 F). Together, these results demonstrate that interactions between membrane proteins can be detected with antibody-mediated FRET in situ and establish that differences in the assembly status of abundantly expressed resident ER membrane proteins can be easily discriminated.

Because some models of translocon dynamics posit small, conformational changes rather than gross assembly and disassembly, we also sought to experimentally determine if small changes in antigen proximity at the low nanometer scale could be reliably discriminated. Because FRET efficiency for a single donor and acceptor dye pair is inversely related to the sixth power of the distance between them (see online supplemental material and references therein), small increases in separation distance markedly reduce the energy transfer. Our simulations suggested that, even for highly flexible antibodies stochastically labeled with multiple dyes, changes in antibody proximities corresponding to even 1 nm should be readily detectable (Fig. S2, available at http://www.jcb.org/cgi/content/full/jcb.200312079/DC1). To assess this experimentally, we exploited an antibody against a different, NH_2-terminal epitope on the lumenal domain of CNX. Although the proximity of CNX to Sec61β yields a relatively low overall FRET signal (consistent with a separation distance of ~10 nm), we asked if changing the donor antibody position from the COOH to the NH_2 terminus on CNX could be detected as a change in FRET. Remarkably, this relatively subtle repositioning of the donor antibody with respect to Sec61β_{Cy5} (Fig. 2 D) decreased the FRET efficiency by nearly half of that seen with the COOH-terminal antibody (Fig. 2, E and F).

Positioning the donor antibody still further away from the COOH terminus of CNX (by using the 2°$_{Cy3}$ donor bound to an unlabeled CNX COOH-terminal antibody) decreased the FRET efficiency to near background levels (Fig. 2, E and F). Based on the dimensions of the unlabeled spacer IgG, we infer that the 2°$_{Cy3}$ donor antibody could be at most 15 nm further from the acceptor than a directly labeled CNX $_{Cy3}$ COOH-terminal donor. Thus, antibody-based FRET is sufficiently sensitive to detect changes in distance in the size range of individual proteins, roughly 1–15 nm. These distances are particularly relevant to the objectives of this paper because the translocon dimensions fall within this range. In addition, two ribosome-bound translocons are sterically blocked from coming closer than 25 nm to each other (Fig. S3 B, available at http://www.jcb.org/cgi/content/full/jcb.200312079/DC1), indicating that intertranslocon FRET should not be detectable by antibody-based FRET. Thus, both theoretical predictions (Kubitscheck et al., 1993; Kenworthy and Edidin, 1998; online supplemental material) and the donor moving experiments (Fig. 2, E and F) provided confidence that antibody-based FRET was sensitive enough to measure both gross and subtle changes in the organization of components within translocons.

The Sec61 complex assembles into oligomers in cells

Purified Sec61 complex, both in solution (Hanein et al., 1996) and when bound to a eukaryotic ribosome (Menetret et al., 2000; Beckmann et al., 2001), is capable of forming ~10-nm-diam toroidal structures estimated to contain at least three copies of the Sec61 heterotrimer. However, demonstrating the stoichiometry of the Sec61 complex in native translocons has proven more difficult to address. By cryo-EM, native channel complexes were larger, had a differently shaped and larger central pore, and contained a substantial lumenal protrusion not seen with Sec61p channels (Menetret et al., 2000; Morgan et al., 2002). Because a ribosome engaged in translocation tightly associates with several other membrane proteins comparable in abundance with the Sec61 complex (Gorlich et al., 1992; Matlack and Walter, 1995; Menetret et al., 2000), the composition and stoichiometry of the components that define the native translocation channel remain uncertain.

To determine if native translocons contain Sec61 oligomers, we asked whether or not FRET could be observed between two copies of a Sec61 complex subunit by labeling cells with a mixture of Sec61β_{Cy3} and Sec61β_{Cy5} antibodies at a relative ratio of 1:8. If homooligomers exist, each copy of the donor-labeled Sec61β is likely to be adjacent (within 10–15 nm) to a copy of the far more numerous acceptor-labeled antibodies. In contrast, a single Sec61 complex per translocon should result in an inter-Sec61β distance, even within polysomes, of at least 25 nm, a distance beyond which little or no FRET is observed. Thus, the ~17% FRET efficiency for Sec61β_{Cy3}/Sec61β_{Cy5} pair (Fig. 3 A) provides direct evidence that native translocons in cells are composed of at least two Sec61 heterotrimers.

Direct comparisons of the FRET efficiency for Sec61β_{Cy3}/Sec61β_{Cy5} with that observed between Sec61α and Sec61β_{Cy5} provided additional support for this conclusion. Here, directly conjugated Sec61α donor antibodies displayed a FRET efficiency to Sec61β_{Cy5} higher than that seen with Sec61β_{Cy3}/Sec61β_{Cy5} (~30% vs. ~17%; Fig. 3, A and B). In contrast, spacing the donor antibody using an unlabeled Sec61α antibody showed a lower FRET efficiency (~7%; Fig. 3 C). Because the spacer antibody dimensions are at most 15 nm and the Sec61β_{Cy3}/Sec61β_{Cy5} FRET efficiency is bracketed between the FRET values for directly conjugated Sec61α and that seen with the spacer antibody, we conclude that one copy of Sec61β must be within ~15

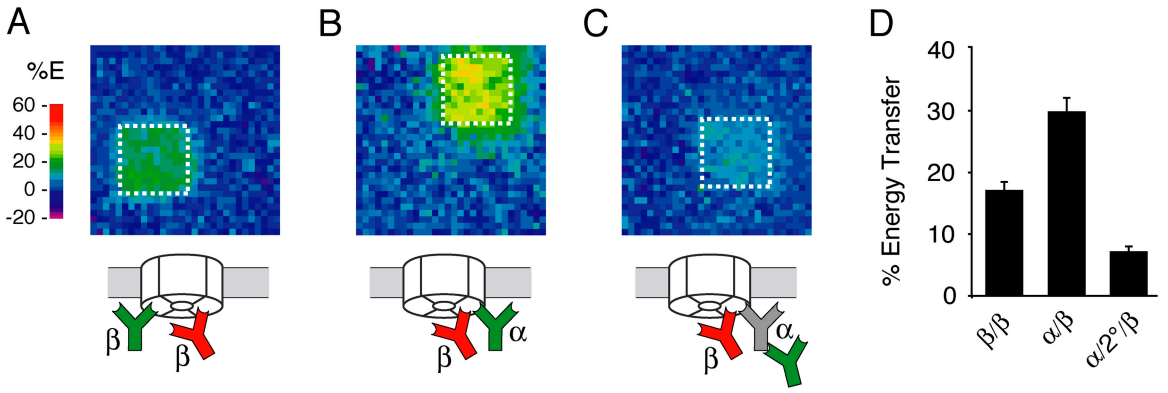

Figure 3. **Detection and characterization of Sec61 complex oligomerization in situ.** (A–C) Direct comparisons of FRET efficiencies to $Sec61\beta_{Cy5}$ from three different donor antibodies: $Sec61\beta_{Cy3}$ (at a ratio of 1:8; A), $Sec61\alpha_{Cy3}$ (B), and $2°_{Cy3}$ bound to unlabeled anti-Sec61α (C). (D) Quantitation (mean ± SD; $n = 10$) of the comparisons from A–C are shown.

nm of another copy. In other experiments, $Sec61\alpha_{Cy3}$/$Sec61\alpha_{Cy5}$ also displayed comparably high FRET (see the following section; Table I), providing additional evidence for oligomeric Sec61 heterotrimers. These values are consistent with the estimated dimensions of native translocons (Menetret et al., 2000) and theoretical simulations of antibodies separated by roughly 8–10 nm (see online supplemental material). Together, these results strongly argue that the observed FRET for $Sec61\beta_{Cy3}$/$Sec61\beta_{Cy5}$ and $Sec61\alpha_{Cy3}$/$Sec61\alpha_{Cy5}$ is detecting oligomerized Sec61 complexes within native translocons. Thus, the data in Figs. 2 and 3 not only demonstrate that protein–protein interactions within the translocon can be detected with high resolution in cells but that the proximities of copies of a subunit of the Sec61 complex can be used to directly probe its oligomeric status.

Core translocon organization during the transport cycle

These results permitted us to simply and directly address a long-standing unresolved issue regarding the dynamics of the translocon: what happens to the translocation channel when it is not actively engaged in substrate transport? To resolve this question, we first established conditions to complete translocation by terminating protein synthesis either prematurely with puromycin, which releases nascent polypeptides from the ribosome, or naturally with pactamycin, an inhibitor of translational initiation. Pulse labeling of cells treated with 1 mM puromycin demonstrated that within 5 min, the synthesis of radiolabeled proteins longer than ~50–70 residues was effectively inhibited due to premature termination. Pactamycin also inhibits new protein synthesis within 5 min, but as expected for an inhibitor of initiation, an additional 10 min was required to complete translation of already engaged mRNAs (Fig. 4 A). Importantly, >95% of the translocons were bound to ribosomes in a salt-resistant manner, whereas <5% remained bound if cells were pretreated with puromycin (Fig. 4 B). Because the high salt containing solubilization conditions used in the fractionation studies maintain ribosome–translocon interactions only in the presence of a nascent chain (Gorlich et al., 1992; Jungnickel and Rapoport, 1995), this result demonstrates that the vast majority of translocons are engaged in translocation in untreated cells, whereas they are nearly quantitatively vacated upon treatment with puromycin (or pactamycin; unpublished data).

Next, we investigated whether or not the oligomeric state of the Sec61 complex in cells was maintained or lost upon the completion of substrate translocation by measuring FRET between all combinations of Sec61α and Sec61β under the two extremes of translocon usage and quiescence. Ten independent FRET measurements were performed on separate cells that were either treated with puromycin or pactamycin or left untreated (Fig. 4, C–F). For each antibody pair, the FRET efficiencies were comparable for actively engaged versus nontranslocating translocons. Importantly, our observation that in untreated cells, the majority of Sec61α or Sec61β labeling is dependent on RNase digestion (Fig. S1) suggests that we are indeed visualizing and making measurements on engaged translocons. Thus, the finding of comparable FRET values after puromycin and pactamycin treatments suggests that the oligomeric structure of active translocons is maintained even after completion of substrate translocation. Therefore, we conclude that the core of a native translocation channel does not disassemble into its individual components upon completion of substrate transport in vivo.

What then distinguishes an engaged from a quiescent translocon? As discussed in the Introduction, the translocon could be structurally identical in both cases (Menetret et al., 2000) or could undergo a conformational change (Hamman

Table I. **Changes in Sec61 complex configuration during the translocation cycle**

Donor	Acceptor	Untreated	Puromycin	Pactamycin
Sec61α	Sec61α	38.3 ± 4.4	33.6 ± 7.2[a]	35.5 ± 5.1[a]
Sec61α	Sec61β	26.4 ± 2.1	27.9 ± 2.7[a]	28.0 ± 2.1[a]
Sec61β	Sec61α	41.8 ± 3.1	46.1 ± 2.8[a]	46.8 ± 3.0[a]
Sec61β	Sec61β	21.4 ± 3.6	24.8 ± 6.1[a]	23.9 ± 2.5[a]

FRET efficiencies (mean ± SD; $n = 40$) for the indicated donor–acceptor antibody pairs were measured on cells that were either left untreated or pre-treated for 15 min with 1 mM puromycin or 0.2 μM pactamycin. Each value is the mean of measurements collected from four separate experiments performed on multiple days.

[a]Treatment is significant ($P \leq 0.01$) compared with untreated cells using *t* test.

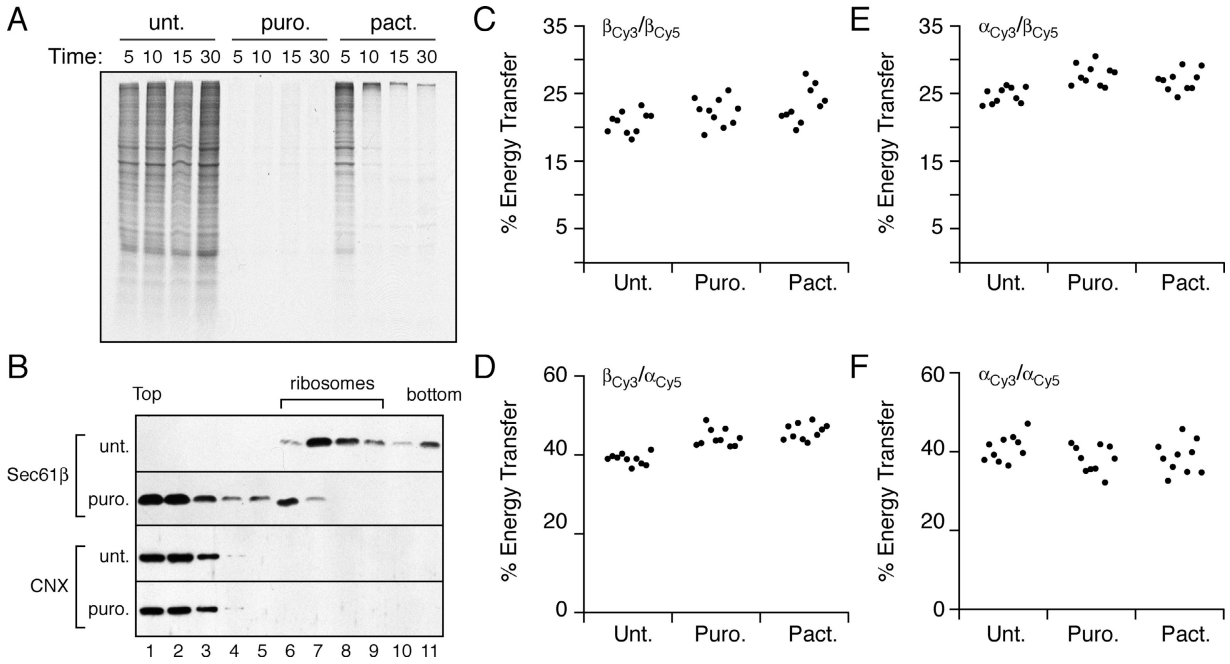

Figure 4. **Translocon component organization during the translocation cycle.** (A) MDCK cells were either left untreated (unt.) or pretreated with 1 mM puromycin (puro.) or 0.2 μM pactamycin (pact.) for the indicated times before pulse labeling for 10 min with [^{35}S]methionine in the presence of the drug. Shown are autoradiographs of total cell lysates. Coomassie blue staining of the gel revealed equal amounts of total protein in each lane (not depicted). (B) Untreated or puromycin-treated (1 mM for 15 min) cells were lysed in detergent (0.8% deoxyBigCHAP) and high salt (500 mM KAc) and analyzed by sucrose density gradient sedimentation for Sec61 complex association with ribosomes. Shown are immunoblots for Sec61β and CNX of individual fractions of the gradient. The position of ribosomes on the gradient is indicated. (C–F) Untreated, puromycin-treated, and pactamycin-treated cells were analyzed for FRET between Sec61β_{Cy3}/Sec61β_{Cy5}, Sec61β_{Cy3}/Sec61α_{Cy5}, Sec61α_{Cy3}/Sec61β_{Cy5}, and Sec61α_{Cy3}/Sec61α_{Cy5} as indicated. Each point on the graph represents a single FRET measurement performed as in Fig. 1 D. $n = 10$ for each condition tested.

et al., 1997; Beckmann et al., 2001). Because antibody-mediated FRET, in principle, can discriminate even small differences in the distances separating antigens, we used this method to determine if a change in organization distinguishes translocating from quiescent translocons in cells. Careful examination of the data in Fig. 4 hinted at small, systematic differences in FRET efficiencies for some of the antibody pairs upon completion of translocation. This possibility was verified with more thorough analyses compiling 40 independent FRET measurements of engaged versus inactive translocons for each antibody pair. Statistical comparisons of untreated versus treated cells revealed small but significant differences for each of the donor/acceptor pairs (Table I).

Several observations suggest that the changes in FRET are specific and reflect the changes in organization that distinguish engaged and inactive translocons. First, the level of antibody labeling was not different for either Sec61α or Sec61β in untreated versus puromycin or pactamycin treated cells (Fig. S1, E and F). This finding argues against changes in FRET due simply to differential labeling or antibody accessibility. Second, two qualitatively different methods of vacating the translocon shift the FRET value in the same direction (either up or down) for each of the four antibody pairs tested. In addition, the lack of statistically significant differences between puromycin and pactamycin treatments for any antibody pair argues that both methods of completing translocation are equivalent from the standpoint of the structural state achieved by the Sec61 components. Third, the FRET values for the reciprocal antibody pairs Sec61α_{Cy3}/Sec61β_{Cy5} and Sec61β_{Cy3}/Sec61α_{Cy5} similarly increase upon completion of translocation, as would be expected for simply switching the donor and acceptor fluorophores on the same antibodies. The difference in the absolute FRET values observed for Sec61α_{Cy3}/Sec61β_{Cy5} versus Sec61β_{Cy3}/Sec61α_{Cy5} is likely due to small differences in dyes per antibody for the different antibody preparations and the efficiency of antigen occupancy for the two antibodies (Fig. S4). Fourth, the increase in FRET for Sec61β_{Cy3}/Sec61β_{Cy5} with a concomitant decrease for Sec61α_{Cy3}/Sec61α_{Cy5} argues against additional or fewer Sec61 heterotrimers being assembled into oligomers. Instead, this result, coupled with the increased FRET for both Sec61α_{Cy3}/Sec61β_{Cy5} and Sec61β_{Cy3}/Sec61α_{Cy5}, is most consistent with the preexisting oligomerized Sec61 complexes undergoing a small but detectable change in configuration.

TRAM, TRAP, and SR associations with translocons

If the core translocon remains intact throughout the translocation cycle, what happens to proteins that do not necessarily stably associate with the translocon, and yet are essential for discrete steps of translocation? To address this question, we focused on three proteins, SRα, TRAM, and TRAPα, each of which are thought to be needed during early stages of translocation. Whether or not they are needed at stages after the initiation of substrate translocation remains unclear. Similarly, it is not known if they are recruited to translocons tran-

Table II. **Maintenance of translocon component interactions during the translocation cycle**

Donor	Acceptor	Untreated	Puromycin	Pactamycin
SRα	Sec61α	34.1 ± 5.2	31.6 ± 7.3	32.2 ± 4.2
SRα	Sec61β	16.0 ± 2.2	17.2 ± 3.3	18.8 ± 2.8[a]
TRAPα	Sec61α	18.4 ± 6.4	13.6 ± 5.6[a]	15.2 ± 4.9
TRAPα	Sec61β	13.6 ± 3.5	11.1 ± 3.1[a]	11.8 ± 2.7
TRAM	Sec61α	17.6 ± 4.2	19.8 ± 2.9[a]	19.7 ± 4.4
TRAM	Sec61β	12.8 ± 2.7	11.9 ± 2.0	10.4 ± 1.1[a]

FRET efficiencies for the indicated donor–acceptor antibody pairs were measured and tabulated as in Table I.
[a]Treatment is significant ($P \leq 0.01$) compared with untreated cells using *t* test.

siently in a use-dependent manner (e.g., as CNX is thought to be) or if they instead are more stably part of the translocon structure (e.g., as are subunits of the Sec61 complex).

We reasoned that these possibilities should be discernible with FRET in two ways. First, FRET between each component and the Sec61 complex under conditions of ongoing translocation may reveal whether, at steady-state, a significant proportion of the proteins are associated with the core translocon or not. Second, if their associations are use- or substrate-dependent, relieving translocons of their substrates with puromycin or pactamycin should result in a loss of FRET signal. Analysis of FRET between SRα, TRAM, and TRAPα donor antibodies with $Sec61\alpha_{Cy5}$, and to a lesser extent $Sec61\beta_{Cy5}$, revealed FRET efficiencies higher than that seen with a CNX donor (Table II; compare for example with Fig. 2, B–D). Instead, many of the FRET efficiencies were more comparable to that seen between subunits of the Sec61 complex (Table I). It should be noted that the systematically lower FRET values seen with the Sec61β acceptor (Table II) appear to be due to small differences in dyes per IgG for the different antibody preparations and do not necessarily indicate a higher distance separating the antigens. That notwithstanding, the data suggest that at steady state, at least some proportion of SRα, TRAM, and TRAPα is likely to be part of Sec61-containing translocons.

However, the absolute amounts of SR, TRAM, and TRAP that are incorporated into translocons are difficult to judge based on the FRET results alone. For the TRAP complex, previous biochemical analyses have demonstrated that the vast majority is tightly associated with membrane-bound ribosomes (Gorlich and Rapoport, 1993; Matlack and Walter, 1995), which is consistent with a high degree of incorporation into translocons. Similar observations for TRAM and SR are lacking because under the conditions analyzed any potential association that might have existed in intact membranes was not maintained upon detergent solubilization. However, our observation that SRα and TRAM gave quantitatively similar FRET values as TRAPα for both the Sec61α and Sec61β acceptors may suggest that, in cells, a comparably high percentage of all three components is incorporated into active translocons.

Upon puromycin or pactamycin treatment of cells, many FRET pairs in Table II underwent a small but statistically significant change, with no FRET pair decreasing to <70% of that seen in untreated cells. In some cases, the FRET efficiencies even increased slightly. In every case, the FRET values changed (either increased or decreased) in the same direction for both puromycin- and pactamycin-treated cells, although not all achieved statistical significance presumably due to an insufficiently large sample size. That notwithstanding, the relative lack of change in FRET among the components analyzed in Table II suggests that a significant degree of disassembly does not occur on completion of substrate translocation. If the majority of these components is incorporated into translocons in untreated cells (as is argued in the previous two paragraphs), these results would suggest that the close proximity of most SRα, TRAM, and TRAPα to the Sec61 complex is an inherent feature of translocon structure and not a consequence of a translocating substrate.

Discussion

In this work, we have used FRET between directly labeled antibodies to address several basic issues of protein translocon organization and composition in mammalian cells. These experiments have allowed us to draw three principal conclusions regarding translocons in vivo that had either not been addressed or had yielded conflicting results with previous approaches. First, in cells fixed at steady state, while growing under metabolically active conditions, the vast majority of Sec61 complexes are assembled into oligomeric structures. Second, these structures, while remaining oligomeric, undergo a change in configuration between rounds of protein translocation. Third, SR, TRAM, and TRAP do not appear to significantly change their associations with the Sec61 complex after completion of substrate translocation. These findings have several implications for translocation, each of which is briefly discussed in the following paragraphs.

The decisive step in cotranslational protein translocation is the achievement of a stable ribosome–translocon complex in which the nascent chain has access to the ER lumen, is shielded from the cytosol, and has committed to forward translocation (Crowley et al., 1994; Jungnickel and Rapoport, 1995; Voigt et al., 1996; Fons et al., 2003). Because completion of protein synthesis or initiation of nascent chain folding before achieving this committed stage results in a cytoplasmically localized substrate (Perara et al., 1986), the precommitment steps in translocation face severe temporal constraints. Additional constraints in vivo include a crowded cellular environment (Luby-Phelps et al., 1986), the large size and low diffusional mobility of ribosome–nascent chain complexes (Rolls et al., 2002), and a potentially limited availability of unengaged components in metabolically active cells (Fig. 4 B). How these constraints are efficiently overcome despite requiring the coordinated actions of up to five components (SRP, SR, TRAM, and the Sec61 and TRAP complexes) has been unclear.

The targeting of nascent chains to the ER includes a transient SRP-mediated slowdown in translation, which provides one mechanism for overcoming the temporal constraints on initiating translocation (Walter and Johnson, 1994). However, later steps, including transfer to the translocon, insertion of nascent chains into the channel, and initiation of translocation, do not appear to involve such translational pauses. We now provide evidence suggesting that these posttargeting steps may be spatially coupled by preas-

sembled translocon structures that are present even before their engagement by a substrate. We suggest that this permits sequential interactions to occur in rapid succession due to the close and constant proximity of the necessary components. Thus, an initial temporal checkpoint (SRP-mediated pausing), together with spatial coupling of the remaining steps, can ensure high fidelity and efficiency of translocation despite the various obstacles posed in vivo.

Currently, it is not known how the various translocon components remain associated in vivo given that biochemical studies have yet to reveal stable associations between them. One possibility is that the conditions required to solubilize the translocon components disrupt interactions that are more stable in the context of an intact lipid bilayer. A more intriguing possibility is that a nontranslating ribosome, which can bind stably to the Sec61 complex under physiologic salt conditions (Kalies et al., 1994), provides a platform for maintaining translocon complexes in an assembled state. For example, it was recently suggested that SR may be close to the translocon (Wittke et al., 2002) and may interact directly with the ribosome (Mandon et al., 2003), which may remain translocon-bound even in the absence of ongoing translocation (Potter and Nicchitta, 2002; Nikonov et al., 2002). If ribosomes indeed do not detach from translocons after substrate translocation, then the lack of significant disassembly of translocon components between rounds of transport (Tables I and II) may be due to an organizing function imparted by the bound ribosome. Thus, the more complete disassembly observed on ER solubilization in vitro requiring high salt-mediated removal of ribosomes from translocons may not normally occur between rounds of transport in vivo. Further studies will be needed to determine the molecular basis of the maintenance of close proximities among the translocon components revealed in this work.

Materials and methods

Antibodies

Antipeptide rabbit antisera against Sec61β, SRα, and TRAPα have been described previously (Fons et al., 2003). Antipeptide antiserum against the COOH termini of canine Sec61α and TRAM were gifts from K. Kellaris and R. Gilmore (University of Massachusetts School of Medicine, Worcester, MA) and K. Matlack and P. Walter (University of California, San Francisco, San Francisco, CA). Rabbit antisera against residues 575–593 (in the COOH-terminal tail of canine CNX) and against residues 50–68 (near the NH_2 terminus of canine CNX) were obtained from StressGen Biotechnologies. The IgG fraction from each of these antibodies was purified by protein A chromatography and labeled using Cy3 or Cy5 monoreactive dye packs (Amersham Biosciences) with slight modifications to the manufacturer's instructions. In brief, 3 mg IgG (in 0.9 ml PBS) was mixed with 0.1 ml 1 M $NaHCO_3$ (pH 9.0) and added to one vial of the dye pack. After 20 min with occasional mixing, the reaction was terminated by separation of the IgG from unreacted dye by Sephadex G-25 chromatography in PBS. This procedure results in the reliable conjugation of ~3.5–4.5 dyes/IgG. Conjugated antibodies falling outside this range were not used. Cy3-conjugated anti–rabbit IgG was obtained from Jackson ImmunoResearch Laboratories and contained an average of ~2.5 dyes/IgG. HRP-conjugated secondary antibodies were obtained from Amersham Biosciences.

Cell culture and sample preparation

MDCK cells were grown in DME containing 10% FBS and glutamine. For imaging, cells were grown in fibronectin-coated 8-chambered Lab-Tek glass coverslips (Nunc) to 40–70% confluence. Translational inhibition (1 mM puromycin; Calbiochem) or 0.2 mM pactamycin (a gift from E. Steinbrecher, Pharmacia Corp., Peapack, NJ) was performed for 15 min at 37°C before fixation. Cells were fixed with 3.7% formaldehyde in PBS for 15 min at RT, washed with PSS (PBS with 10% FBS, 0.1% saponin), and blocked 1 h at RT with PSS containing 50 μg/ml RNase A. Three different labeling protocols were used depending on the configuration of antibodies desired. In experiments where two directly labeled primary antibodies were used, the Cy3- and Cy5-conjugated antibodies were premixed before incubating with cells. In experiments where the $2°_{Cy3}$ donor antibody was bound directly to the acceptor antibody, labeling was performed sequentially. After binding the Cy5-labeled antibody as aforementioned, the cells were washed before binding the Cy3-labeled secondary antibody. In experiments using an unlabeled "spacer" antibody to which the $2°_{Cy3}$ donor antibody was bound, labeling was performed in multiple steps. First, the unlabeled primary antibody was bound, after which the cells were washed, before binding $2°_{Cy3}$. After washing, the samples were fixed with 3.7% formaldehyde. Any remaining antigen binding sites on the secondary antibody were blocked with PBS containing 5% rabbit serum and 0.1% saponin, and subsequently incubated with the Cy5-conjugated antibodies. After completion of each of the labeling protocols, samples were washed and the cells were either viewed immediately or postfixed in 3.7% formaldehyde (which had no effect on the FRET observed) before rinsing into PSS for imaging.

Microscopy and image analysis

Images were acquired with a confocal microscope (model LSM-510; Carl Zeiss MicroImaging, Inc.) using a 1.4 NA 63× oil objective using 543 and 633 nm HeNe laser lines with 560–615 and 650 filters with open pinholes. Complete photobleaching of Cy5 was accomplished by 125 iterative scans with 5 mW illumination at zoom 4. Images were collected sequentially in the Cy3 and Cy5 channels immediately before and after photobleaching a region. FRET quantitation and generation of the energy transfer map were automated using custom macros (available upon request) written for NIH Image 1.62. Two experiments confirmed the specificity of donor dequenching. Acceptor-only labeled samples ensured no bleed-through into the donor channel. A donor-only labeled sample was shown to not change in intensity upon bleaching in the acceptor channel under the bleach conditions used.

Biochemical analyses

Lysates from MDCK cells for immunoblots (Fig. S1 A) were prepared in 100 mM Tris, pH 8, 500 mM KAc, 5 mM $MgCl_2$, and 1% Triton X-100. After removing any insoluble material (10 min at maximum speed in a microcentrifuge), the proteins were precipitated with 15% TCA, washed in acetone, and analyzed by SDS-PAGE and immunoblotting. Canine pancreatic rough microsomal membranes were solubilized directly in SDS-PAGE sample buffer and analyzed by immunoblotting. For metabolic labeling, cells growing in 12-well dishes at ~70% confluence were treated with translational inhibitors in methionine-free media for between 5–30 min before the addition of [^{35}S]methionine/cysteine Translabel (ICN Biochemicals) to 100 μCi/ml. After 10 min of labeling at 37°C, cells were rinsed once in PBS, solubilized in 100 μl 1% SDS/0.1 M Tris (pH 8.0), and heated in a boiling water bath, and a 5-μl aliquot was analyzed by SDS-PAGE and autoradiography. For sucrose gradient analysis, a 6-well dish containing cells at ~70% confluence was transferred to ice, rinsed in ice-cold PBS, and scraped into 500 μl of ice-cold 50 mM Hepes, pH 7.4, 500 mM KAc, 5 mM $MgAc_2$, 0.8% deoxyBigCHAP (Calbiochem), and 1 mM DTT. Cells were solubilized by repeated passage through a small-bore pipette tip and sedimented at 10,000 *g* for 10 min in a refrigerated microcentrifuge, and 200 μl of the supernatant was applied to a 2-ml 10–50% (wt/vol) sucrose gradient containing the solubilization buffer. After centrifugation for 1 h at 55,000 rpm in a TLS-55 rotor (Beckman Coulter), 11 fractions were removed and the proteins precipitated with TCA and analyzed by immunoblotting. Fractions containing ribosomes were identified in separate gradients by monitoring absorbance at 260 nm or Coomassie blue staining of the fractions.

Miscellaneous

SDS-PAGE was performed on 12% Tris-tricine gels. Immunoblotting was performed after transfer to nitrocellulose and development was with Supersignal chemiluminescence reagents (Pierce Chemical Co.). Figures were assembled using Photoshop and Illustrator software (Adobe).

Online supplemental material

Nine supplemental figures, accompanying text, and figure legends are available online. These provide additional experimental characterization of the FRET methodology (Figs. S1 and S7–S9) and theoretical analyses of ensembles of fluorophores conjugated to antibodies (Figs. S2–S6). Online

supplemental material is available at http://www.jcb.org/cgi/content/full/jcb.200312079/DC1.

We thank A. Kenworthy, G. Patterson, P. Randazzo, and D. Lowy for helpful discussions; K. Kellaris and R. Gilmore for antisera against Sec61α; K. Matlack and P. Walter for antisera against TRAM; and C. Nicchitta for advice on the acquisition and use of pactamycin.

E.L. Snapp was a Pharmacology Research Associate Program fellow. This work was supported by the intramural programs of the National Cancer Institute and National Institute of Child Health and Human Development.

Submitted: 10 December 2003
Accepted: 17 February 2004

References

Beckmann, R., D. Bubeck, R. Grassucci, P. Penczek, A. Verschoor, G. Blobel, and J. Frank. 1997. Alignment of conduits for the nascent polypeptide chain in the ribosome-Sec61 complex. *Science.* 278:2123–2126.

Beckmann, R., C.M.T. Spahn, N. Eswar, J. Helmers, P.A. Penczek, A. Sali, J. Frank, and G. Blobel. 2001. Architecture of the protein-conducting channel associated with the translating 80S ribosome. *Cell.* 107:361–372.

Bergeron, J.J., M.B. Brenner, D.Y. Thomas, and D.B. Williams. 1994. Calnexin: a membrane-bound chaperone of the endoplasmic reticulum. *Trends Biochem. Sci.* 19:124–128.

Crowley, K.S., S. Liao, V.E. Worrell, G.D. Reinhart, and A.E. Johnson. 1994. Secretory proteins move through the endoplasmic reticulum membrane via an aqueous, gated pore. *Cell.* 78:461–471.

Fons, R.D., B.A. Bogert, and R.S. Hegde. 2003. Substrate-specific function of the translocon-associated protein complex during translocation across the ER membrane. *J. Cell Biol.* 160:529–539.

Gorlich, D., and T.A. Rapoport. 1993. Protein translocation into proteoliposomes reconstituted from purified components of the endoplasmic reticulum membrane. *Cell.* 75:615–630.

Gorlich, D., S. Prehn, E. Hartmann, K.U. Kalies, and T.A. Rapoport. 1992. A mammalian homolog of Sec61p and SecYp is associated with ribosomes and nascent polypeptides during translocation. *Cell.* 71:489–503.

Hamman, B.D., J.C. Chen, E.E. Johnson, and A.E. Johnson. 1997. The aqueous pore through the translocon has a diameter of 40-60 Å during cotranslational protein translocation at the ER membrane. *Cell.* 89:535–544.

Hamman, B.D., L.M. Hendershot, and A.E. Johnson. 1998. BiP maintains the permeability barrier of the ER membrane by sealing the lumenal end of the translocon pore before and early in translocation. *Cell.* 92:747–758.

Hanein, D., K.E. Matlack, B. Jungnickel, K. Plath, K. Kalies, K.R. Miller, T.A. Rapoport, and C.W. Akey. 1996. Oligomeric rings of the Sec61p complex induced by ligands required for protein translocation. *Cell.* 87:721–732.

Jackson, V. 1999. Formaldehyde cross-linking for studying nucleosomal dynamics. *Methods.* 17:125–139.

Johnson, A.E., and M.A. van Waes. 1999. The translocon: a dynamic gateway at the ER membrane. *Annu. Rev. Cell Dev. Biol.* 15:799–842.

Jungnickel, B., and T.A. Rapoport. 1995. A posttargeting signal sequence recognition event in the endoplasmic reticulum membrane. *Cell.* 82:261–270.

Kalies, K.U., D. Gorlich, and T.A. Rapoport. 1994. Binding of ribosomes to the rough endoplasmic reticulum mediated by the Sec61p-complex. *J. Cell Biol.* 126:925–934.

Kenworthy, A.K. 2001. Imaging protein-protein interactions using fluorescence resonance energy transfer microscopy. *Methods.* 24:289–296.

Kenworthy, A.K., and M. Edidin. 1998. Distribution of a glycosylphosphatidylinositol-anchored protein at the apical surface of MDCK cells examined at a resolution of <100 Å using imaging fluorescence resonance energy transfer. *J. Cell Biol.* 142:69–84.

Kubitscheck, U., R. Schweitzer-Stenner, D.J. Arndt-Jovin, T.M. Jovin, and I. Pecht. 1993. Distribution of type I Fc epsilon-receptors on the surface of mast cells probed by fluorescence resonance energy transfer. *Biophys. J.* 64: 110–120.

Luby-Phelps, K., D.L. Taylor, and F. Lanni. 1986. Probing the structure of cytoplasm. *J. Cell Biol.* 102:2015–2022.

Mandon, E.C., Y. Jiang, and R. Gilmore. 2003. Dual recognition of the ribosome and the signal recognition particle by the SRP receptor during protein targeting to the endoplasmic reticulum. *J. Cell Biol.* 162:575–585.

Matlack, K.E., and P. Walter. 1995. The 70 carboxyl-terminal amino acids of nascent secretory proteins are protected from proteolysis by the ribosome and the protein translocation apparatus of the endoplasmic reticulum membrane. *J. Biol. Chem.* 270:6170–6180.

Menetret, J.F., A. Neuhof, D.G. Morgan, K. Plath, M. Radermarcher, T.A. Rapoport, and C.W. Akey. 2000. The structure of ribosome-channel complexes engaged in protein translocation. *Mol. Cell.* 6:1219–1232.

Molinari, M., and A. Helenius. 2000. Chaperone selection during glycoprotein translocation into the endoplasmic reticulum. *Science.* 288:331–333.

Morgan, D.G., J. Menetret, A. Neuhof, T.A. Rapoport, and C.W. Akey. 2002. Structure of the mammalian ribosome-channel complex at 17 Å resolution. *J. Mol. Biol.* 324:871–886.

Nikonov, A.V., E. Snapp, J. Lippincott-Schwartz, and G. Kreibich. 2002. Active translocon complexes labeled with GFP-Dad1 diffuse slowly as large polysome arrays in the endoplasmic reticulum. *J. Cell Biol.* 158:497–506.

Perara, E., R.E. Rothman, and V.R. Lingappa. 1986. Uncoupling translocation from translation: implications for transport of proteins across membranes. *Science.* 232:348–352.

Potter, M.D., and C.V. Nicchitta. 2002. Endoplasmic reticulum-bound ribosomes reside in stable association with the translocon following termination of protein synthesis. *J. Biol. Chem.* 277:23314–23320.

Rapoport, T.A., B. Jungnickel, and U. Kutay. 1996. Protein transport across the eukaryotic endoplasmic reticulum and bacterial inner membranes. *Annu. Rev. Biochem.* 65:271–303.

Rolls, M.M., D.H. Hall, M. Victor, E.H. Stelzer, and T.A. Rapoport. 2002. Targeting of rough endoplasmic reticulum membrane proteins and ribosomes in invertebrate neurons. *Mol. Biol. Cell.* 13:1778–1791.

Roy, A., and W.F. Wonderlin. 2003. The permeability of the endoplasmic reticulum is dynamically coupled to protein synthesis. *J. Biol. Chem.* 278:4397–4403.

Simon, S.M., and G. Blobel. 1991. A protein-conducting channel in the endoplasmic reticulum. *Cell.* 65:371–380.

Van den Berg, B., W.M. Clemons, Jr., I. Collinson, Y. Modis, E. Hartmann, S.C. Harrison, and T.A. Rapoport. 2004. X-ray structure of a protein-conducting channel. *Nature.* 427:36–44.

Voigt, S., B. Jungnickel, E. Hartmann, and T.A. Rapoport. 1996. Signal sequence–dependent function of the TRAM protein during early phases of protein transport across the endoplasmic reticulum membrane. *J. Cell Biol.* 134:25–35.

Walter, P., and A.E. Johnson. 1994. Signal sequence recognition and protein targeting to the endoplasmic reticulum membrane. *Annu. Rev. Cell Biol.* 10: 87–119.

Wang, L., and B. Dobberstein. 1999. Oligomeric complexes involved in translocation of proteins across the membrane of the endoplasmic reticulum. *FEBS Lett.* 457:316–322.

Wittke, S., M. Dünnwald, M. Albertsen, and N. Johnsson. 2002. Recognition of a subset of signal sequences by Ssh1p, a Sec61p-related protein in the membrane of endoplasmic reticulum of yeast *Saccharomyces cerevisiae. Mol. Biol. Cell.* 13:2223–2232.

JCB
Online Supplemental Material

Snapp et al. http://www.jcb.org/cgi/doi/10.1083/jcb.200312079

Theory, modeling, and simulations of FRET between dye-conjugated antibodies

Fluorescence resonance energy transfer (FRET) refers to the nonradiative transfer of energy from an excited "donor" fluorescent molecule to an "acceptor" molecule. Although a wide variety of parameters influences the probability of FRET (Matyus, 1992; Clegg, 1995; Wouters, et al., 2001), the most important are the distance separating the donor and acceptor, and their respective fluorescence spectra. The dyes Cy3 and Cy5 are a well-characterized donor-acceptor pair whose probability of FRET is 50% when separated by ~5 nm (Bastiaens and Jovins, 1996). Because FRET efficiency is inversely dependent on the sixth power of the distance separating the donor and acceptor, it is a highly sensitive measure of even small (subnanometer) changes in the relative proximities of the dyes. For a single donor and acceptor fluorophore, the probability of FRET on excitation of the donor is $1/[1+(r/R_o)^6]$, where r is the distance separating the fluorophores and R_0 is the distance at which a 50% probability of FRET is observed (the so called Förster distance; Förster, 1948).

In this work, very large and highly flexible antibody probes conjugated in multiple random positions with fluorescent dyes were used to measure FRET. Previously, antibody-based FRET has been used to analyze protein–protein interactions in vivo

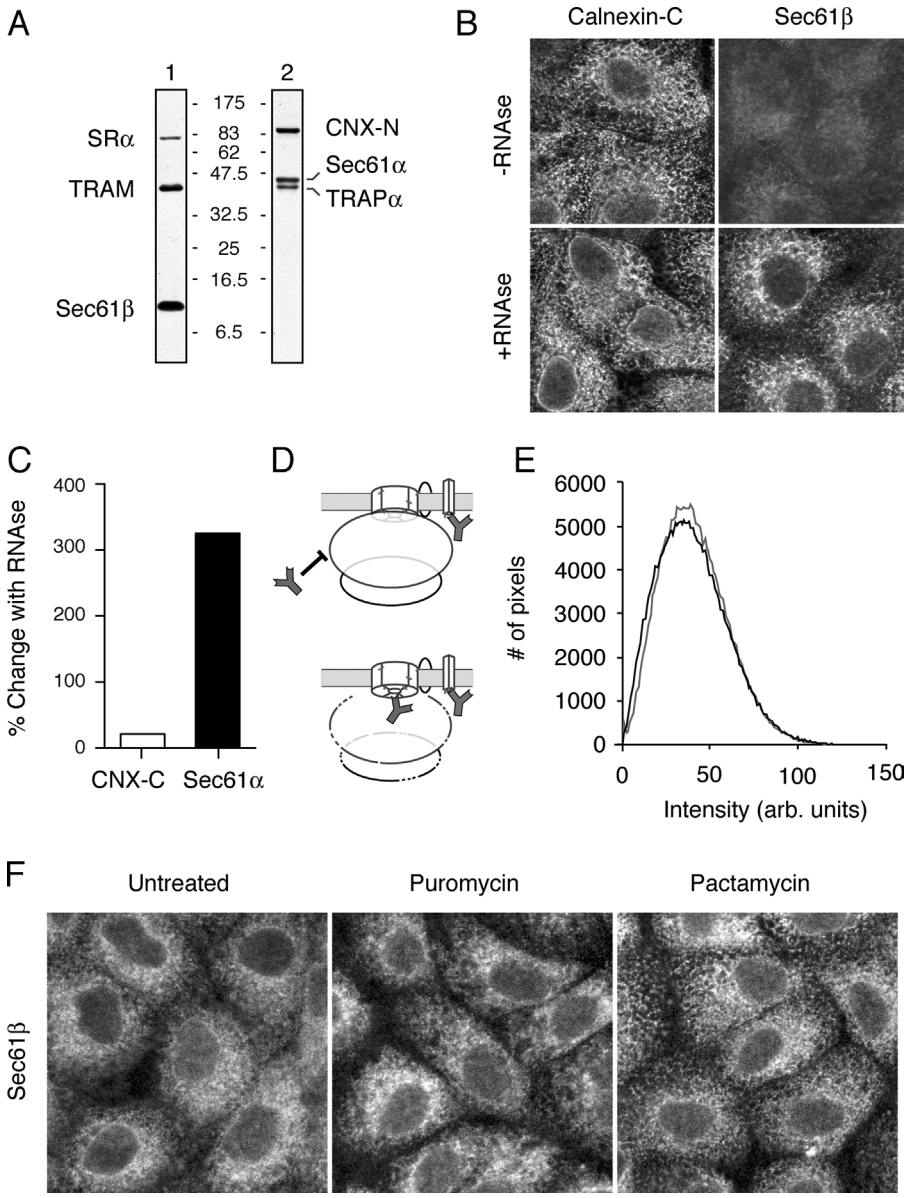

Figure S1. **Characterization of antibody labeling of MDCK cells.** (A) Immunoblots of MDCK cell lysates. Lane 1 was probed with a mixture of antibodies against Sec61β, TRAM, and SRα. Lane 2 used antibodies against TRAPα, Sec61α, and the NH_2 terminus of CNX. The positions of individual proteins and molecular weight markers are indicated. (B) Fixed andpermeabilized cells were either left untreated (top) or digested for 1 h with 50 μg/ml RNase at RT (bottom) before incubation with directly conjugated antibodies against the COOH terminus of CNX (left) or Sec61β (right). Images without and with RNase digestion were taken with identical settings. Similar results were obtained for Sec61α, quantitation of which showed an ~3-fold increase in fluorescence, whereas CNX in the same samples (using a different colored antibody) showed no significant change (C). (D) Schematic diagram depicting the observed results for accessibility of antibodies to core translocon components versus another ER protein in the presence (top) or absence (bottom) of RNase. The red hatches indicate that the samples are fixed and immobilized, and therefore do not reorganize upon partial digestion of the ribosome (indicated by the dotted line). (E) Shown are the distributions of fluorescence intensities for a field of cells that were either untreated (black) or puromycin treated before fixation, digestion with RNase, and staining with Cy3-conjugated Sec6α antibodies. Note that the total staining with antibody and distribution of fluorescence intensities are very similar. Similar results were obtained for the Sec61β antibody, which also showed equal efficiencies of antibody accessibility in RNase-digested cells that were either untreated or pretreated with puromycin or pactamycin before fixation (F).

(Bastiaens et al., 1996; Kenworthy, 2001; Haj et al., 2002) and to discriminate between randomly distributed and clustered cell surface proteins (Kubitscheck et al., 1993; Kenworthy and Edidin, 1998). Because oligomeric assembly and disassembly of a multiprotein complex is conceptually equivalent to a "clustered" versus "nonclustered" state, we reasoned that similar principles might be applied to examine translocon assembly. However, the dimensions of the antibody probes (~14 nm; Fig. S2 A) are substantially larger than the distances over which FRET occurs, and the number and distribution of dyes on the antibody surface are random. Furthermore, the antibodies, as well as the dyes conjugated to them, are flexible enough to substantially influence their absolute positions. These and other variables complicate the relationship between the observed FRET and the distance separating the antigens to which donor and acceptor antibodies are bound (Dewey and Hammes, 1980; Haas and Steinberg, 1984). Thus, the appropriate design and interpretation of experiments depend upon a careful consideration of the theoretical expectations. Therefore, we modeled and directly simulated FRET between antibodies with varying parameters such as density of antigens, relative ratios of donor to acceptor antibodies, percent occupancy of antigens by antibodies, and configuration of antigens (e.g., randomly distributed vs. assembled into "clusters" of defined size). Monte Carlo simulations, rather than theoretical calculations using simplifying assumptions, were used to provide insight into not only the expected FRET efficiency but also the degree of variability that can be anticipated from measurement to measurement due to the stochastic nature of many of the variables involved (Haas and Steinberg, 1984).

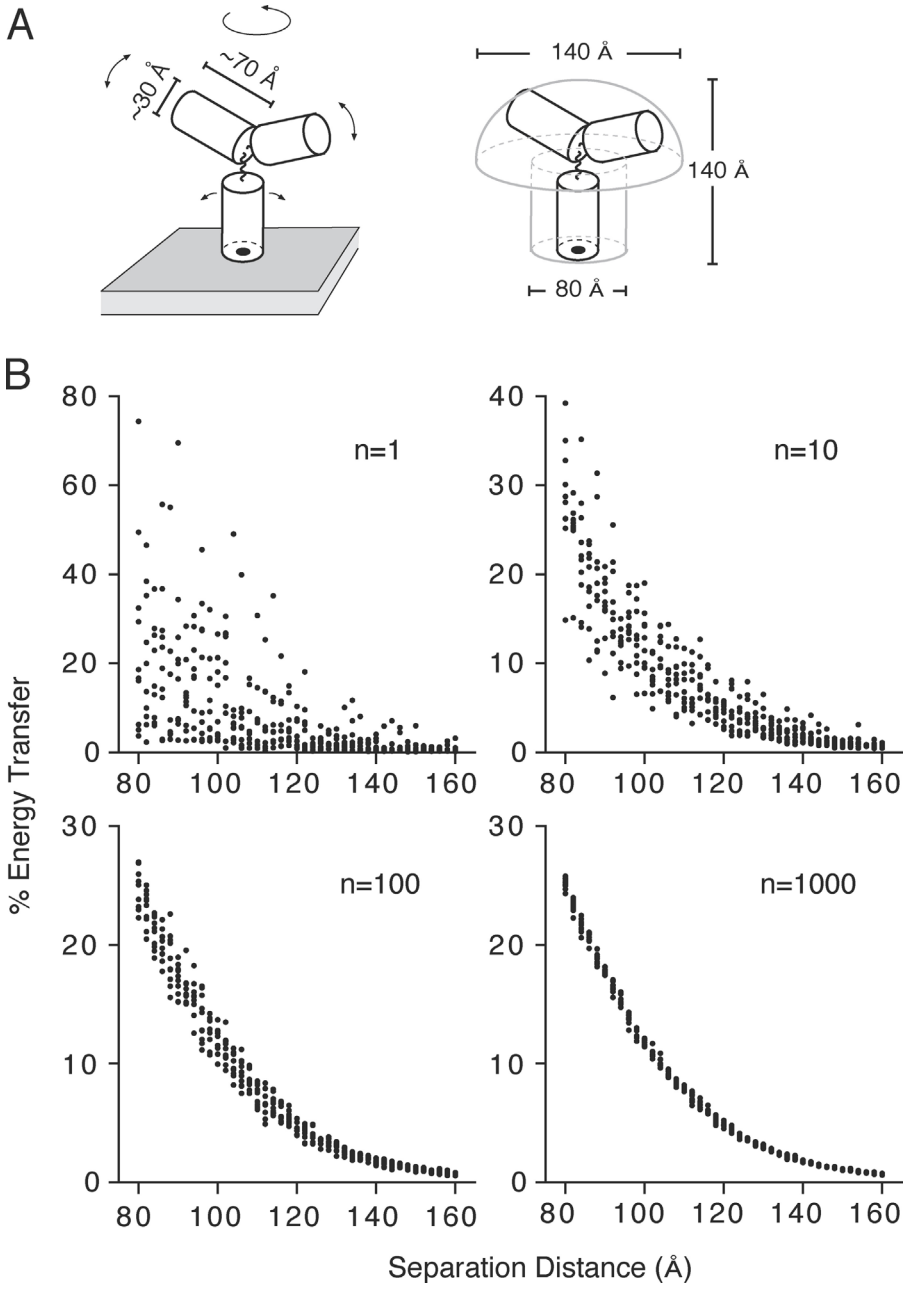

Figure S2. **Sampling size and the resolving power of antibody-mediated FRET.** (A) Diagram of a model IgG molecule bound to an antigen on the membrane surface (left). The Fc and each Fab domain are modeled as a cylinder of 3-nm diameter, 7 nm height, connected by flexible hinges. Arrows indicate directions of allowed rotational flexibility. The range of potential positions that can be occupied by dyes conjugated to the antibody surface is indicated on the right. Dyes are allowed to be on the surface of the "stalk" of the mushroom-shaped space and anywhere in the volume of the "head." (B) A simulated donor- and acceptor-labeled antibody (4 dyes/IgG, randomly distributed as described in A) were bound to antigens separated by distances of between 8 and 16 nm, and the FRET between the dyes calculated and plotted. Each datum represents the average of between 1 and 1,000 such simulations as indicated on each graph.

Antibodies were modeled as three cylindrical domains (one Fc and two Fab domains), each of 3-nm diameter and 7-nm length, connected by flexible hinge regions (Fig. S2 A). Dyes were assumed to be capable of being distributed randomly on the surface of this structure. When one Fab domain is bound to an antigen on a membrane surface, the other two domains are torsionally and rotationally flexible. Thus, dyes on these nonbound domains can essentially occupy any potential position in a large hemisphere of ~14-nm diam. Dyes on the bound Fab domain, due to more limited flexibility, were modeled as occupying the surface area of a 7-nm-high cylinder of 8-nm diameter.

Using these parameters for placing dyes randomly with respect to the antigen position, simulations were used to assess FRET between a donor and acceptor antibody bound to antigens separated by defined distances (ranging from 8 to 16 nm). For these simulations, four dyes for both the donor and acceptor antibody were positioned randomly within the volume they could potentially occupy based on the above parameters. Once the donor and acceptor dye positions were set using this stochastic method, the expected FRET efficiency for this particular ensemble of fluorophores was calculated according to previously established equations (Dewey and Hammes, 1980). The first graph of Fig. S2 B ($n = 1$) shows a scatter plot of the range of FRET values obtained for any single antibody pair separated by various distances. At a separation distance of 8 nm, the FRET efficiencies ranged broadly from <5% to nearly 80% (Fig. S2 B, $n = 1$). This tremendous variability reflects the stochastic distributions of the donor and acceptor dyes over a large volume, combined with the extreme sensitivity of FRET to small changes in the distances separating them. Indeed, it has been shown previously that if the number of sampled molecules is small, such dramatic fluctuations can be anticipated (Haas and Steinberg, 1984).

Although a trend is observed in which increased separation distance between the antibodies results in lower FRET, a single interaction cannot be used to discriminate different antigen positions (except to say that antigens are either within ~15 nm of each other or further away). However, the resolving power increases substantially as more antibody pair interactions are sampled and averaged (Fig. S2 B, $n = 10$ through $n = 1{,}000$). At a sampling size of 1,000, differences in separation distance of between 0.2–0.4 nm can be resolved with confidence. Thus, subnanometer changes in antigen separation can be resolved using FRET between dye-conjugated antibodies despite the highly flexible and large nature of the probes, the stochastic distribution of the dyes bound to them, and the complex relationships for FRET between ensembles of donor and acceptor fluorophores.

Therefore, we modeled the use of antibody-mediated FRET to probe the structure and organization of a multiprotein structure such as the translocon. It is important to note that although we have applied the general principles arising from the following simulations to interpret our experimental results, the models are not intended to accurately model the physical structure of a translocon. Rather, they serve to illustrate the capabilities, sensitivity, and specificity of this approach and provide boundaries for the type of questions that can be addressed. In particular, two issues are of direct relevance to our studies: (1) the discrimination of assembled from disassembled multiprotein (or oligomeric) complex, and (2) the discrimination of small changes in the structure of a complex that remains assembled in the same general configuration. Both of these issues can be explored using a simplified structure that does not necessarily reflect the full complexity of the native

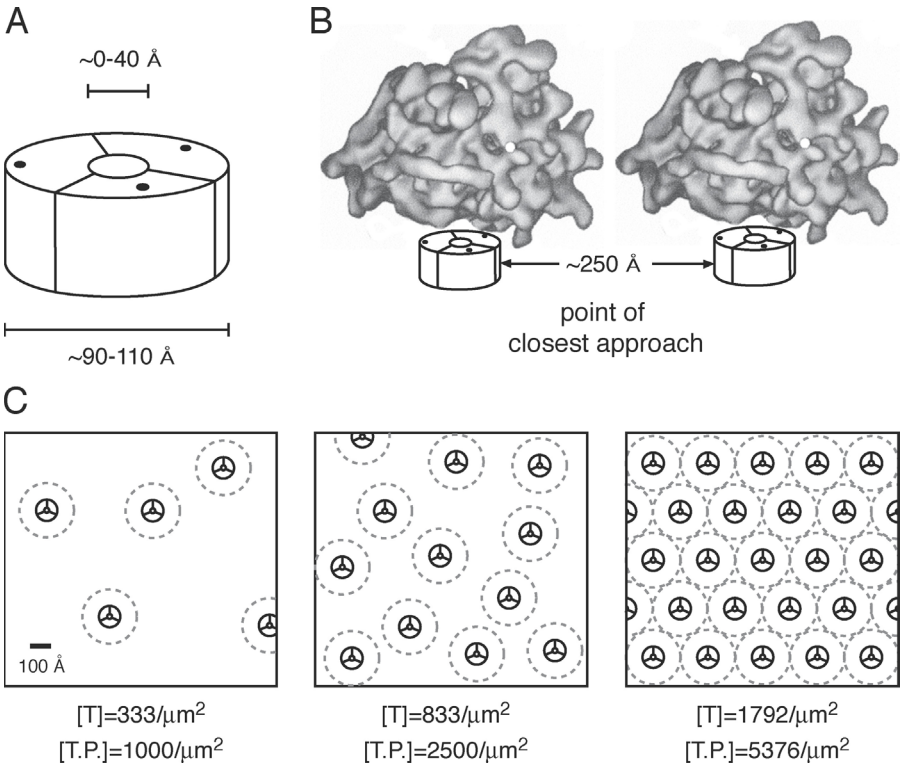

Figure S3. **Estimated size and densities of the translocon.** (A) An idealized translocon protein (such as Sec61β; indicated by a black dot) was modeled in the simulations as being present in the assembled translocon as three copies distributed around a toroid with a diameter of between 9 and 11 nm. (B) The point of closest approach of two translocons engaged in translocation is restricted by the size of the bound ribosome, which is at least 25 nm in width. The model of the mammalian ribosome is based on cryo-EM reconstructions (Morgan, et al., 2002) and is shown relative to a translocon of ~10-nm diam. (C) Ribosome-bound translocons on a membrane surface at various densities are shown in a scale diagram. The ribosome is indicated by a 25-nm-diam dotted circle, with translocons in the center. The surface densities of translocons (T) and a translocon protein (T.P.) present as three copies per translocon are indicated below each diagram. The diagram on the right represents the upper limit for translocon density based on the maximum packing of ribosomes on a membrane surface.

translocon. Therefore, we used a simplified model system comprising a hypothetical protein capable of assembling into oligomeric units of three. Simulations of antibody-mediated FRET for changes in the oligomeric status and/or configuration of this model system, which is based only loosely on an idealized translocon, could nonetheless be used to assess the potential utility of this method to address the aims of this present work. The details of this model system were guided by the currently available data on translocon size, structure, and abundance in the ER membrane.

Based on electron microscopy data (Hanein et al., 1996; Beckmann et al., 1997, 2001; Menetret et al., 2000), an idealized translocon was modeled as a cylinder of diameter between 9 and 11 nm (Fig. S3 A). Three copies of a translocon protein (e.g., Sec61β) that serve as "antigens" for potential antibody binding were distributed equally around the periphery of this idealized translocon. Estimates for the density of translocons in the ER ranged from ~200 to ~1500/μm^2. These estimates were guided by the observations that most translocons appear to be ribosome bound at steady state (Gorlich et al., 1992; Matlack and Walter, 1995; Potter and Nicchitta, 2002; Nikonov et al., 2002; see Fig. 4 B from main text), and the principal translocon components (such as the Sec61 complex) appear to be comparable in abundance to membrane-bound ribosomes (Gorlich, et al., 1992; Gorlich and Rapoport, 1993). Because 25 nm spheres (roughly the size of the ribosome) cannot be packed on a membrane surface at densities >1792/μm^2 (Fig. S3, B and C), this marks the maximum achievable density of membrane-bound ribosomes, and hence translocons. Only the most highly secretory cells (such as the exocrine pancreas or plasma cell) would even approach this density of bound ribosomes. Inspection of electron micrographs of a tissue culture cell arrived at an estimate of ~10–15

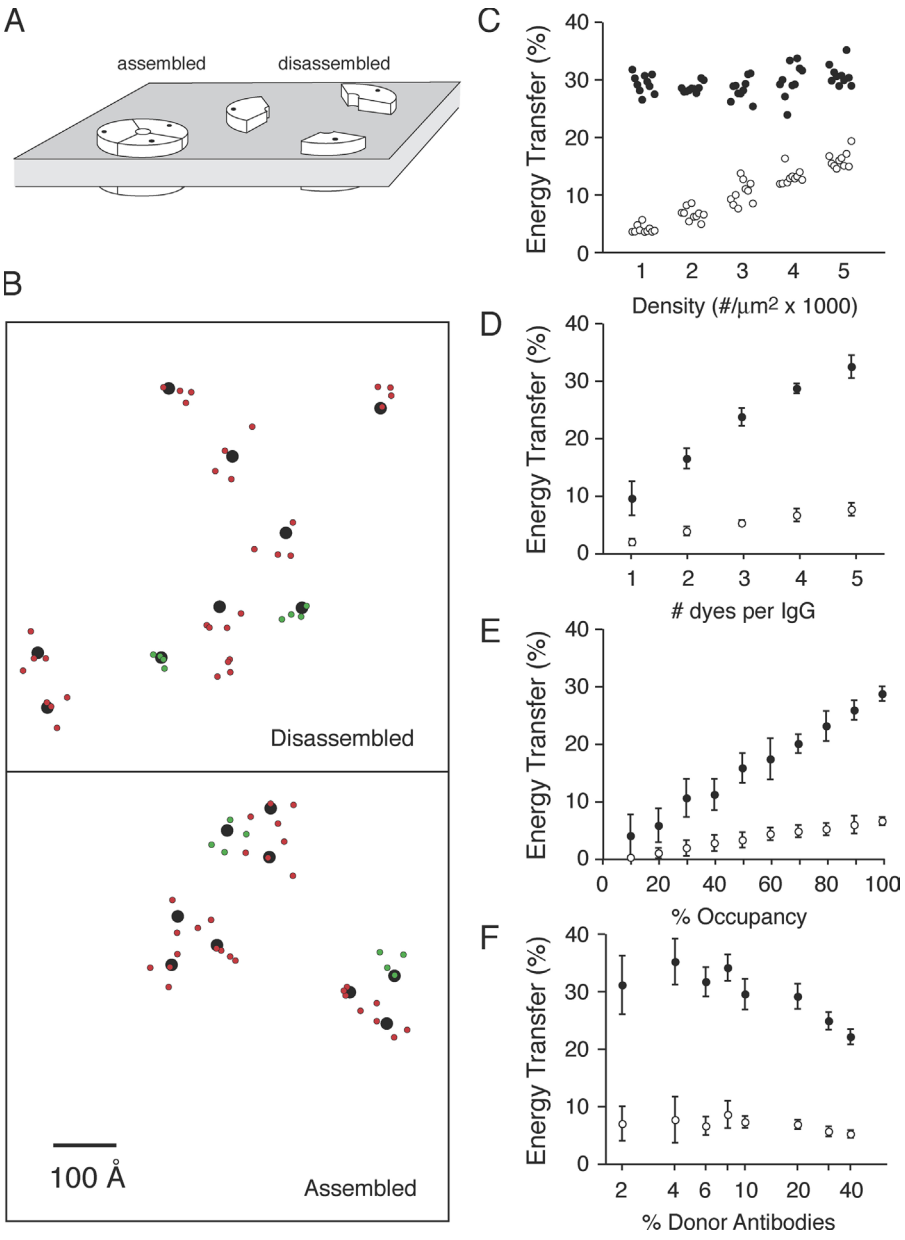

Figure S4. **Simulations of FRET for assembled versus unassembled translocons.** (A) Idealized configurations of an oligomeric channel in the membrane in an assembled and disassembled configuration. The positions of a putative antigen present as three copies in the channel are indicated with a black dot. (B) Surface view of a 70 × 70-nm section of membrane containing antigens (black dots) at 2,000 copies/μm^2 in assembled and disassembled configurations as in A. The two-dimensional projection of the positions of donor (green) and acceptor (red) dyes on antibodies bound to these antigens is also indicated. An antibody was assigned a 20% probability of containing donor dyes. (C) Monte Carlo simulations were used to calculate the FRET efficiencies in a 0.25-μm^2 section of membrane containing donor- and acceptor-labeled antibodies (at a ratio of 1:4, each containing 4 dyes per IgG) bound to antigens (with 100% occupancy) at densities of 1,000 to 5,000 copies/μm^2. The antigens were either randomly distributed or assembled into clusters of three (around a 10-nm circle) that were randomly distributed in the membrane surface (closed circles). The simulation was repeated ten times for each condition, with each point representing the FRET from a single simulation. Note that FRET in the nonclustered configuration displays a clear density dependence that is not seen in the clustered configuration. (D and F) FRET as a function of the number of dyes per IgG, degree of occupancy of the antigen by antibody, and proportion of antibodies that carry donor dyes were simulated as in C. Randomly distributed antigens (open circles) were compared with clustered antigens (closed circles). The mean ± SD of 10 simulations is plotted for each condition. When not being specifically varied, antibodies contained four dyes each, 20% of antibodies were donors, antigen occupancy was 100%, and antigen density was 2,000 copies/μm^2.

ribosomes per linear micrometer of ER membrane (Seiser and Nicchitta, 2000). Extrapolation to a surface would give a modest density of ~200/μm^2, which presumably represents a lower limit for translocon density.

For most simulations, we used a value of ~667 translocons/μm^2 (i.e., 2,000 copies of the translocon protein per μm^2) that we considered a reasonable estimate of the situation in a metabolically active, secretory cultured cell type such as the MDCK cells used in this work. Visual representations of ribosome-bound translocons in a membrane at various densities are shown in Fig. S3 C. We began by simulating the expected FRET values for a random distribution of a translocon protein at various surface densities ranging from 1,000 to 5,000 copies/μm^2. For comparison, we also calculated the corresponding FRET values for these same translocon proteins assembled into "translocons" (i.e., clusters of three proteins arranged in a circle of 10-nm diameter) that were randomly distributed (Fig. S4 A). For these simulations, the probability that an antigen will be occupied with an antibody was set at 100%; the probability that the antibody will contain donor dyes was 20%; and each antibody contained four dyes (arbitrarily distributed as described above). A visual representation of the relative proximities of translocon proteins and fluorescent dyes in the "disassembled" and "assembled" states for a small section of membrane is shown in Fig. S4 B as a 2-dimensional illustration. For each condition to be tested, 10 independent FRET measurements were simulated for 0.25 μm^2 areas and plotted (Fig. S4 C). Several observations are noteworthy. First, at each density, including the unrealistic maximal density of 5,000/μm^2, the assembled (or clustered) configuration was readily distinguishable from the unassembled (or randomly distributed) one. Second, the FRET among the randomly distributed antigens displayed a clear density dependence that was not seen for the clustered situation containing assembled translocons. And third, an area of 0.25 μm^2 (which contains between 250 and 1250 translocon proteins, depending on density) provides a sufficiently large sampling size to not only resolve clustered from unclustered antigens but also differences in FRET due to increasing densities.

A variety of other parameters was also tested systematically, including the number of dyes per antibody (Fig. S4 D), the percent of antigens occupied by the antibody (Fig. S4E), and the ratio of donor to acceptor antibodies (Fig. S4F). Based on these simulations, and on the assumption that a realistic density of a core translocon protein in the ER of a tissue culture cell is at most ~2,000/μm^2, several parameters regarding the experimental setup were chosen. First, the antibodies were labeled with ~4 dyes per IgG to maximize fluorescent signal and FRET efficiency while minimizing the disruption of binding activity. Second, the donor to acceptor ratio was kept at or below 1:4, usually ~1:8. This again maximized FRET efficiency without making the donor fluorescence intensity too dim to easily visualize. Third, to maximize occupancy of antigen with antibody, we used saturating concentrations of antibody and increased the incubation time to two hours to allow complete binding. Moreover, we reduced steric hindrance due to bound ribosomes by treating the fixed, permeabilized cells with RNase before antibody binding. Each of these modifications was found to increase the efficiency of FRET (unpublished data) as would be expected if the occupancy of antigens was improved.

The putative assembled versus disassembled states of the translocon represent the extremes of configurations; thereby making them easily distinguishable by antibody-mediated FRET. Because the active versus inactive configurations of the translocon may instead represent a more subtle change in arrangement of its components, we used the simulations to ask whether or not such small changes could also be distinguished. To model a small change in configuration (Fig. S5 A), the diameter of the translocon was varied from 9 to 11 nm in 0.4-nm increments and the FRET at each size was measured. For these simulations, we used a translocon

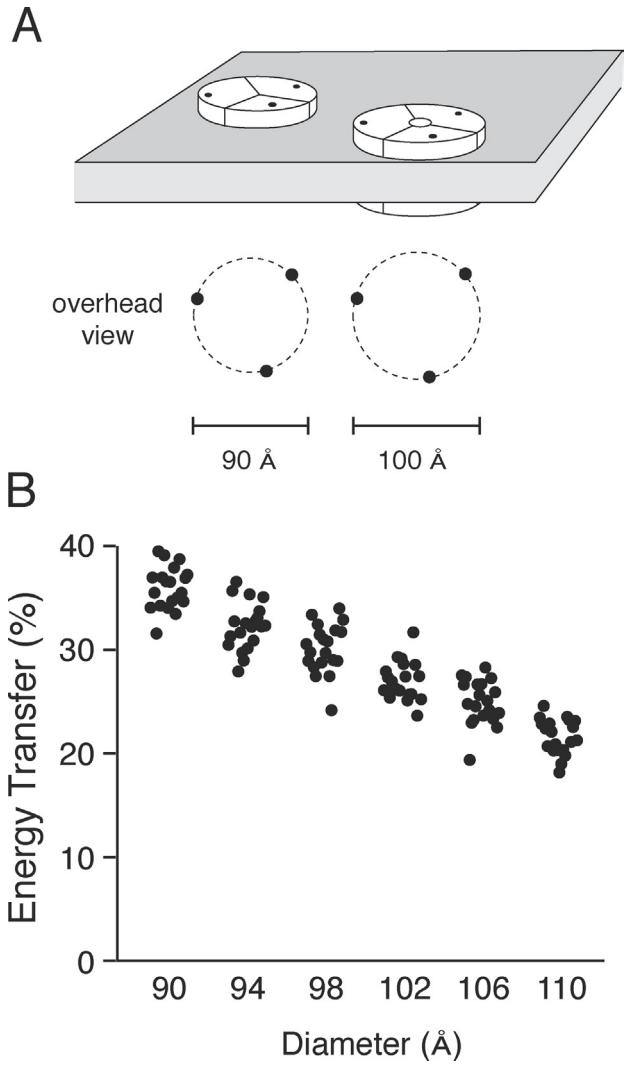

Figure S5. **Simulations of FRET for translocons undergoing a conformational change.** (A) Scale diagram of a translocon of 9- versus 10-nm diameter. A translocon protein is present as a cluster of three antigens around a circle of the indicated diameter. (B) Clusters of three antigens in circles of diameters ranging from 9 to 11 nm were randomly distributed in 0.25 μm^2 areas, and the FRET between the bound antibodies calculated by Monte Carlo simulations as in Fig. S4 C. Each set of 20 measurements was statistically significant ($P < 0.01$) from an adjacent set. The density of antigens was 2,000/μm^2, each IgG contained four conjugated dyes, and 20% of the antibodies contained donor dyes.

protein density of 2,000/μm^2, 4 dyes per antibody, 20% donor antibodies, and 100% occupancy of antigens. As seen in Fig. S5 B, even such small changes can be distinguished given sufficient sampling. Under these conditions, 20 areas of 0.25 μm^2, each containing assemblies at a density of $\sim$667/μm^2 (Fig. S5), was sufficient to distinguish a 0.4-nm difference. This modest sampling size (i.e., a total of $\sim$5 μm^2) represents the lower limit for distinguishing such small changes using idealized conditions. Presumably, parameters like a lower density of assemblies, incomplete antibody labeling, and the experimental imprecision of microscopy-based FRET, and cell-to-cell variability all would require increases in the sampling size to achieve a high resolving power. Nonetheless, given that the translocon components are relatively abundant (Gorlich, et al., 1992; Gorlich and Rapoport, 1993), and that the surface area of the ER within a typical cultured cell is roughly 20,000 μm^2 (Griffiths, et al. 1984), antibody-mediated FRET measurements of small areas within single cells should provide more than enough sampling to reliably measure protein proximity at nanometer resolution.

As noted above, the simple geometry used to simulate a translocon-like structure is not likely to accurately reflect the more complex physical structure of a native translocon. However, the simulations suggested that changes to a multiprotein structure, whether it is simple or complex, are likely to be detectable with antibody-mediated FRET. To directly test this suggestion, we also performed simulations with two other model translocons of different geometry: one that contained four, rather than three, copies of a protein in each structure, and another that contained three copies of one protein and one copy of a different protein intercalated within the structure. We found that regardless of the starting geometry, relatively small changes in structure (in this example, a 1-nm change in diameter) could be readily detected by differences in the FRET (Fig. S6). These results indicate that although different geometries of a translocon can produce different absolute FRET values compared with our idealized translocon, changes within the confines of a different structure are still detectable with antibody-mediated FRET. Thus, antibody-mediated FRET should be a feasible method to monitor both gross and subtle changes in translocon structure in cells.

FRET efficiency and the photoconversion of the Cy5 fluorophore

It was recently reported that upon photobleaching, the Cy5 fluorophore is photoconverted into a fluorescein-like fluorophore that has the potential to confound FRET analyses using the acceptor photobleaching method (Nichols, 2003; unpublished data). This report is particularly relevant if the Cy3 fluorescence is extremely dim relative to Cy5 and/or if the Cy3 excitation light intensity or Cy3 detector gains are set at very high levels. Because of the potential to substantially influence the apparent FRET that is observed, it is important and worthwhile to carefully consider this phenomenon in interpreting our results.

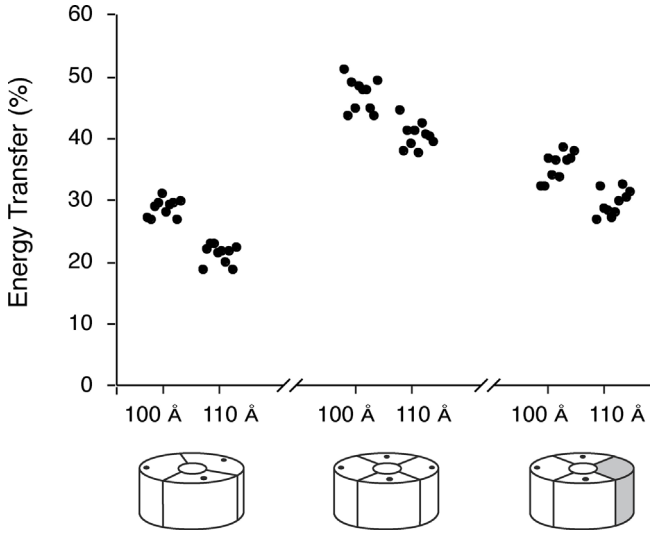

Figure S6. **Translocon geometry and the detection of conformational changes by FRET.** Three different geometries of hypothetical translocons were modeled as indicated below the graph. In addition to the one used in Fig. S5 (left), translocons with four antigens were also constructed. They were composed of either a single antigen (middle) or three copies of one antigen with one copy of another protein that does not serve as an antigen (right). For each geometry, the effect on FRET of changing the diameter of the translocon from 10 to 11 nm is compared as in Fig. S5. Note that in each case, the change in translocon size can be readily detected as a change in the FRET. Interestingly, changes in geometry without changing the size can also be distinguished (e.g., compare each geometry at the 10-nm diameter).

One approach to this problem is to correct for this photoconverted product by using a standard curve (Nichols, 2003). Indeed, in other experiments performed in our lab, this was required because the "FRET" signal was significantly overrepresented due to photoconversion. However, we have chosen for simplicity not to correct the data presented in the present manuscript for two reasons. First, it was determined that photoconversion contributed to less than $\sim$5% of the value of observed FRET signals. Second, the absolute FRET values are far less important to the interpretation of the results than the relative differences obtained for direct comparisons. For example, the absolute FRET values are generally not used to calculate or draw conclusions regarding distances between components; rather, it is the changes in FRET that are used to infer changes in translocon organization or structure.

Further justification for arriving at the correct interpretation of the data without including this correction factor comes from three lines of data. First, our demonstration that while maintaining the Cy5 acceptor constant, changing the position of the donor antibody changes the FRET signal without changing the intensity of either the donor or acceptor argues against a substantial contribution from photoconversion (Fig. 1, E and F, from main text). Second, for many of the experiments, we have plotted FRET as a function of acceptor intensity for different regions of an image (Fig. S7). This demonstrates that FRET efficiency is not dependent on acceptor density and shows that increased FRET is not observed in areas of increased Cy5 staining, as might be predicted if a substantial proportion of the signal were due

to Cy5 photoconversion. In contrast, an artifactual "FRET" signal due to photoconversion shows a direct dependence on Cy5 intensity (Nichols, 2003; unpublished data). Third, we have also examined the effect of decreasing the donor concentration (with constant acceptor concentration) on FRET efficiency (Fig. S8). If photoconversion is contributing significantly to the Cy3 fluorescence measurements, halving the donor concentration will substantially increase the apparent "FRET" signal. This is because the photoconverted product continues to contribute the same amount of fluorescence to the Cy3 measurements. However, the starting donor intensity is decreased. Thus, the photoconverted product will cause the Cy3 measurements to increase by a much higher percent upon Cy5 photobleaching, resulting in erroneously high FRET values. By contrast, genuine FRET without interference from photoconversion should be largely independent of donor intensity and occupancy. In our experiments, we observed that decreasing the donor concentration did not result in an appreciable increase in the FRET signal (Fig. S8 A) despite lower absolute donor intensity (Fig. S8 B). This finding demonstrates that under these imaging conditions, the photoconverted Cy5 product does not contribute significantly to the Cy3 fluorescence measurements.

FRET between directly interacting versus noninteracting antibodies

In much of this study, the antibodies are assumed to not directly interact with each other to generate FRET, but instead simply mark the positions of the antigens against which they are directed. Thus, a FRET signal between antibodies is taken to reflect the proximities of the antigens to which the antibodies are bound, and not to nonspecific interactions among the antibodies themselves. Therefore, it is critical to the interpretation of the results that the antibodies not interact with each other. There are three observations that confirm this point and demonstrate that FRET between translocon component antibodies is due to the close proximities of the translocon components.

First, we directly compared the expected (Fig. S9, A and B) and actual (Fig. S9 C) properties of the FRET we observe between translocon component antibodies and the FRET seen between antibodies that directly interact with each other. We find that FRET between directly interacting antibodies is largely insensitive to changes in concentration of the ac-

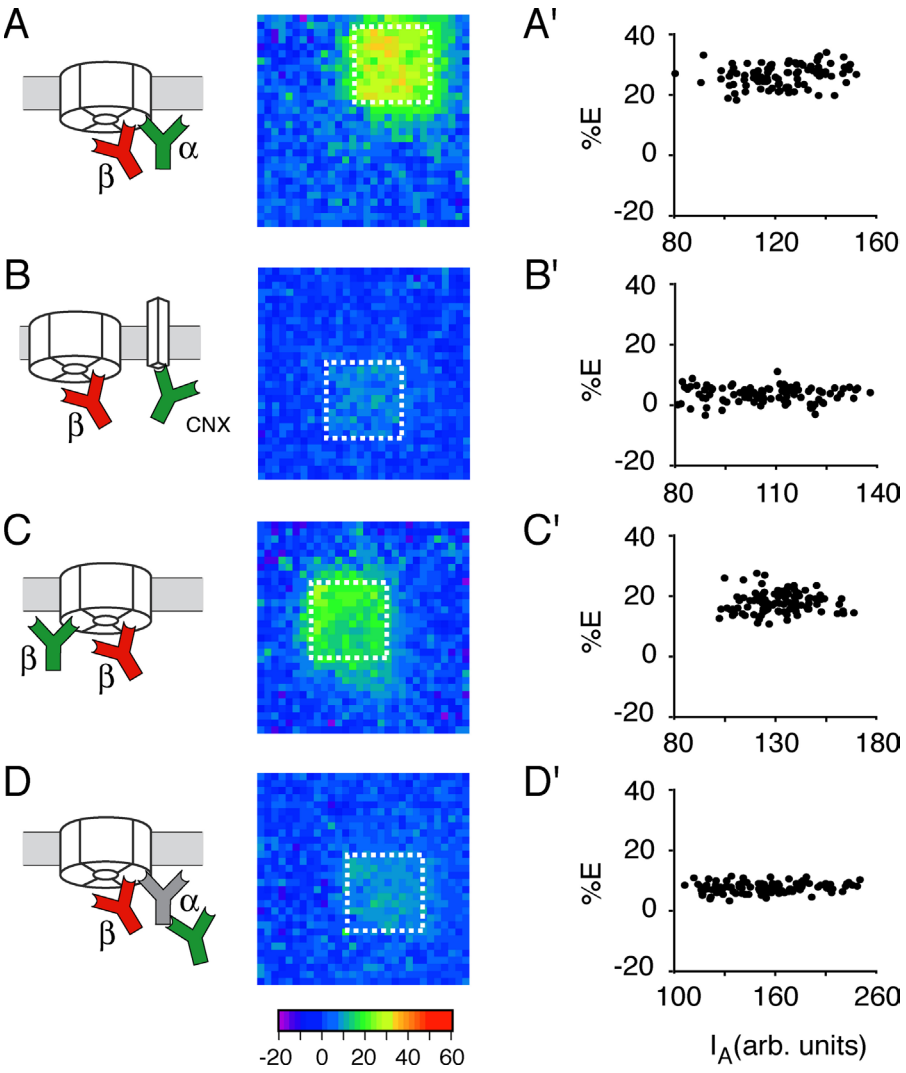

Figure S7. **Relationship between FRET and acceptor fluorescence intensity.** (A–D) Diagrams and energy transfer maps of various images used in other parts of this study. Plotted in the corresponding panels A'–D' is the relationship between intensity of acceptor fluorescence (I_A) and the energy transfer. Each point represents an individual 8 × 8-pixel area within the section of the image analyzed (i.e., bounded by the dotted white box in A-D). Note that the energy transfer efficiency does not change as a function of acceptor intensity.

ceptor antibody (Fig. S9 C). This is because the only donor labeling that occurs is via binding to an acceptor. Thus, although reduced labeling occurs due to the reduced acceptor concentration, all donors are still adjacent to an acceptor, and therefore generate a high FRET signal (Fig. S9 B). In marked contrast, FRET between the translocon component antibodies used in this work is reduced severalfold when the acceptor concentration is reduced (Fig. S9 C). This result is to be expected if the antibodies are interacting with antigens whose proximities bring the antibodies close to each other. Here, the donor antibodies still bind to their antigens, but some of the acceptor antigens will now be unoccupied by acceptor antibodies (Fig. S9 A). The presence of donor antibodies unaccompanied by nearby acceptors should reduce the FRET signal, which is what we have observed experimentally.

In a second type of experiment, we measured FRET between the Sec61α and Sec61β antibodies with and without a peptide competitor corresponding to the antigen for the Sec61β antibody. Inclusion of the peptide during the antibody incubation resulted in both decreased labeling of cells by the Sec61β antibody (but not the Sec61α antibody), and a loss of the FRET signal (unpublished data). Thus, the binding of the antibodies to their antigens, and not nonspecific interactions between the antibodies themselves, is the basis of the FRET signal observed.

Third, we have consistently observed that changing the concentration of one translocon antibody doesn't appreciably change the efficiency of labeling by another translocon antibody in the same sample (unpublished data). Thus, no two of the translocon antibodies interact with each other, but rather just with their antigens. Together, these results demonstrate that we are observing FRET due to the proximities of the antigens to which the antibodies bind and not due to interactions between the antibodies themselves.

Materials and methods

Image analysis

Quantitation of FRET within the photobleached area and generation of the energy transfer map were automated using custom macros (available on request) written for NIH Image 1.62. In brief, the macro performs the following operations in sequence: (1) the pre- and postbleach images are registered to optimal alignment; (2) the area of photobleaching is identified; (3) the percent change in donor intensity (after background subtraction) is calculated in each 8 × 8-pixel region (0.56 × 0.56 μm) of the image and drawn as a pseudocolored map; and (4) the average change within the entire photobleached and nonbleached regions is calculated.

Modeling and simulations

Custom macros (available on request) were written for NIH Image 1.62 to perform the antibody-mediated FRET simulations. In essence, an algorithm was designed to simulate the stochastic binding of a mixture of donor- and acceptor-labeled an-

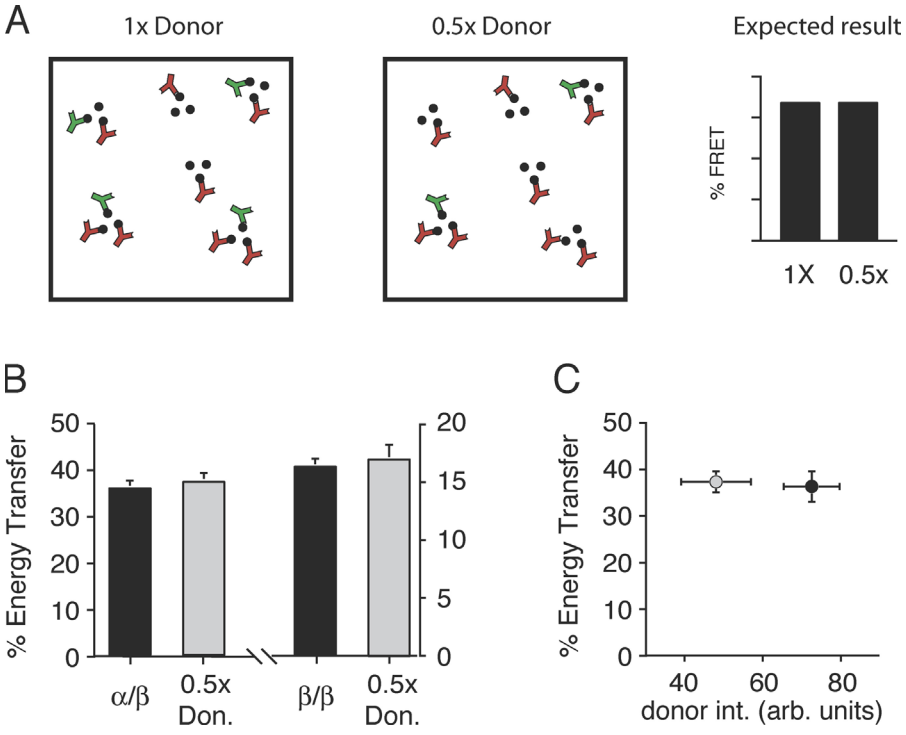

Figure S8. **Independence of FRET on donor concentration and intensity.** (A) Schematic diagram illustrating the effect of donor concentration on FRET. Oligomers of antigens are shown randomly labeled with donor (green) and acceptor (red) antibodies. The right panel contains one half the amount of donor antibody than the left panel. Although the donor fluorescence is expected to be lower for the right panel, the proximity of each donor to acceptor antibodies predicts that FRET efficiency should stay the same. (B) The prediction of the situation in A was experimentally tested by varying the concentration of two different donors ($Sec61\alpha_{Cy3}$ or $Sec61\beta_{Cy3}$) while maintaining the acceptor ($Sec61\beta_{Cy5}$) at a constant concentration. Each histogram represents the mean percentage of energy transfer for FRET measurements of five cells for each experiment. Using a *t*-test ($P \leq 0.01$), no significant differences in energy transfer were detected for the two different donor concentrations. As expected, the overall donor fluorescence intensity decreased upon reducing the donor antibody concentration (C illustrates this for the Sec61α donor; similar results were seen for the Sec61β donor [not depicted]).

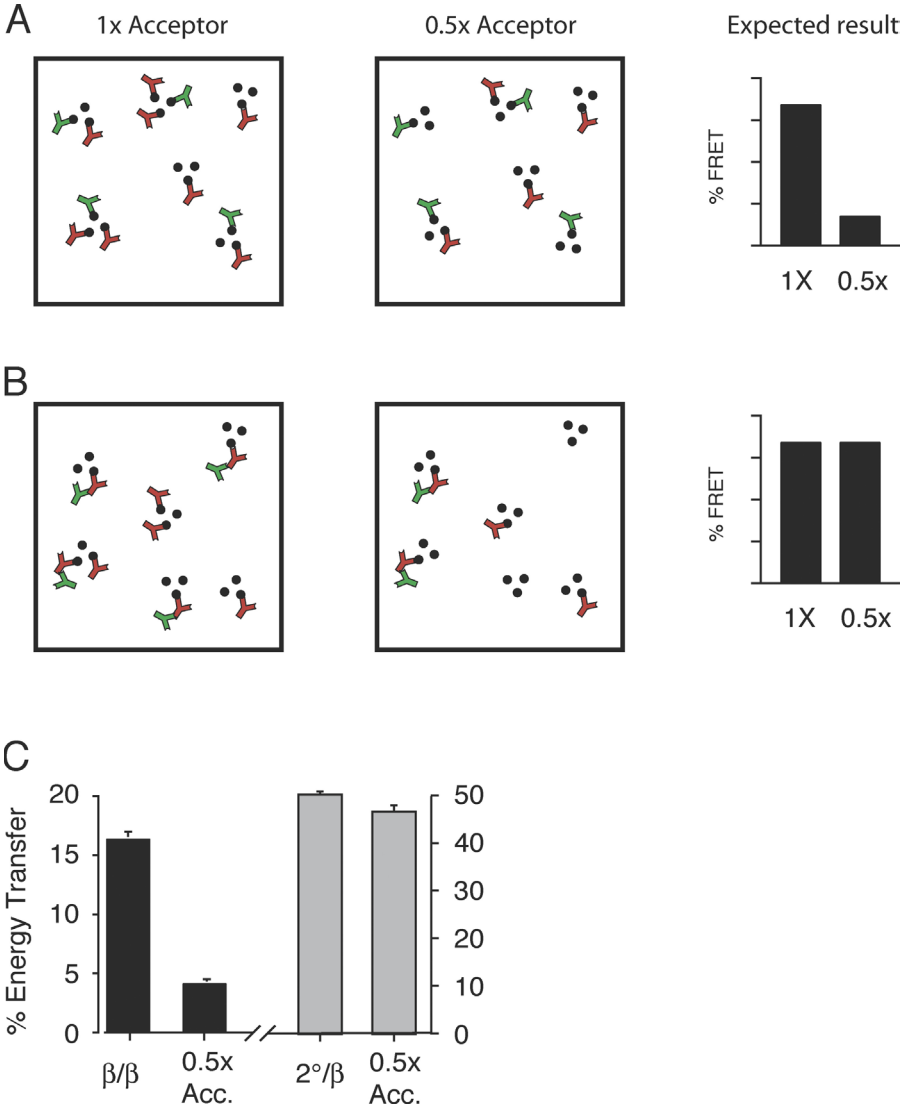

Figure S9. **Dependence of FRET on acceptor concentration.** (A and B) Antibody distributions are illustrated for donor (green) and acceptor (antibodies) on a hypothetical clustered three-antigen oligomer. A shows the situation where the donor and acceptor antibodies bind their antigens, but do not interact with each other. B shows the situation where the acceptor binds its antigen, but the donor antibody interacts with the acceptor antibody. In both cases, the right panel shows the consequence of reducing the acceptor concentration by one half, and the predicted effect on the FRET observed. (C) The prediction from A was tested experimentally by measuring the FRET between a constant amount of $Sec61\beta_{Cy3}$ donor with two concentrations of the $Sec61\beta_{Cy5}$ acceptor. In parallel, the prediction from B was tested using the same $Sec61\beta_{Cy5}$ acceptor at two concentrations, but with a $2°_{Cy3}$ antibody that binds the acceptor antibody directly. As predicted, reducing the acceptor concentration caused no decrease in FRET efficiency for the 2°/β combination, whereas FRET efficiency decreases greater than threefold for the β/β pair.

tibodies to a set of antigens on a membrane surface, followed by a calculation of the FRET between the randomly distributed dyes on all of the bound antibodies. The algorithm encompassed the following steps. First, the x-y positions of the appropriate number of antigens were distributed on a hypothetical surface of defined area (usually $0.5 \times 0.5\mu m$) at the indicated density and configuration (either randomly distributed, or in "clusters" of three). Clusters were not allowed to overlap, and the minimal distance separating adjacent antigens was limited to 8 nm, as determined by the steric hindrance of bound IgG molecules. Second, each antigen was randomly assigned to either be unoccupied, bound by a donor antibody, or bound by an acceptor antibody. The relative probabilities of each assignment were determined by the desired occupancy and donor/acceptor ratio. Third, the x-y-z positions of dyes were randomly chosen relative to each antigen by the criteria outlined in the text. Fourth, once the x-y-z positions for all of the donor and acceptor dyes were set, the summed FRET efficiency that would be expected for this distribution of dyes was calculated according to previously established equations (Förster, 1948; Dewey and Hammes, 1980).

References

Bastiaens, P. I., and T.M. Jovin. 1996. Microspectroscopic imaging tracks the intracellular processing of a signal transduction protein: fluorescent-labeled protein kinase C βI. *Proc. Natl. Acad. Sci. USA.* 93:8407–8412.

Bastiaens, P.I., I.V. Majoul, P.J. Verveer, H.D. Soling, and T.M. Jovin. 1996. Imaging the intracellular trafficking and state of the AB5 quaternary structure of cholera toxin. *EMBO J.* 15:4246–4253.

Beckmann, R., D. Bubeck, R. Grassucci, P. Penczek, A. Verschoor, G. Blobel, and J. Frank. 1997. Alignment of conduits for the nascent polypeptide chain in the ribosome-Sec61 complex. *Science.* 278:2123–2126.

Beckmann, R., C.M.T. Spahn, N. Eswar, J. Helmers, P.A. Penczek, A. Sali, J. Frank, and G. Blobel. 2001. Architecture of the protein-conducting channel associated with the translating 80S ribosome. *Cell.* 107:361–372.

Clegg, R.M. 1995. Fluorescence resonance energy transfer. *Curr. Opin. Biotechnol.* 6:103–110.

Dewey, T.G., and G.G. Hammes. 1980. Calculation on fluorescence resonance energy transfer on surfaces. *Biophys. J.* 32:1023–1035.

Förster, T. 1948. Zwischenmolekulare energiewanderung und fluoreszenz. *Annalen der Physik.* 2:57–75.

Gorlich, D., and T.A. Rapoport. 1993. Protein translocation into proteoliposomes reconstituted from purified components of the endoplasmic reticulum membrane. *Cell.* 75:615–630.

Gorlich, D., S. Prehn, E. Hartmann, K.U. Kalies, and T.A. Rapoport. 1992. A mammalian homolog of Sec61p and SecYp is associated with ribosomes and nascent polypeptides during translocation. *Cell.* 71:489–503.

Griffiths, G., G. Warren, P. Quinn, O. Mathieu-Costello, and H. Hoppeler. 1984. Density of newly synthesized plasma membrane proteins in intracellular membranes. I. stereological studies. *J. Cell Biol.* 98:2133–2141.

Haas, E., and I.Z. Steinberg. 1984. Intramolecular dynamics of chain molecules monitored by fluctuations in efficiency of excitation energy transfer. A theoretical study. *Biophys. J.* 46:429–437.

Haj, F.G., P.J. Verveer, A. Squire, B.G. Neel, and P.I. Bastiaens. 2002. Imaging sites of receptor dephosphorylation by PTP1B on the surface of the endoplasmic reticulum. *Science.* 295:1708–1711.

Hanein, D., K.E. Matlack, B. Jungnickel, K. Plath, K. Kalies, K.R. Miller, T.A. Rapoport, and C.W. Akey. 1996. Oligomeric rings of the Sec61p complex induced by ligands required for protein translocation. *Cell.* 87:721–732.

Kenworthy, A.K. 2001. Imaging protein-protein interactions using fluorescence resonance energy transfer microscopy. *Methods.* 24:289–296.

Kenworthy, A.K., and M. Edidin. 1998. Distribution of a glycosylphosphatidylinositol-anchored protein at the apical surface of MDCK cells examined at a resolution of <100 Å using imaging fluorescence resonance energy transfer. *J. Cell Biol.* 142:69–84.

Kubitscheck, U., R. Schweitzer-Stenner, D.J. Arndt-Jovin, T.M. Jovin, and I. Pecht. 1993. Distribution of type I Fc epsilon-receptors on the surface of mast cells probed by fluorescence resonance energy transfer. *Biophys. J.* 64:110–120.

Matlack, K.E., and P. Walter. 1995. The 70 carboxyl-terminal amino acids of nascent secretory proteins are protected from proteolysis by the ribosome and the protein translocation apparatus of the endoplasmic reticulum membrane. *J. Biol. Chem.* 270:6170–6180.

Matyus, L. 1992. Fluorescence resonance energy transfer measurements on cell surfaces. A spectroscopic tool for determining protein interactions. *J. Photochem. Photobiol. B.* 12:323–337.

Menetret, J.F., A. Neuhof, D.G. Morgan, K. Plath, M. Radermarcher, T.A. Rapoport, and C.W. Akey. 2000. The structure of ribosome-channel complexes engaged in protein translocation. *Mol. Cell.* 6:1219–1232.

Morgan, D.G., J. Menetret, A. Neuhof, T.A. Rapoport, and C.W. Akey. 2002. Structure of the mammalian ribosome-channel complex at 17 Å resolution. *J. Mol. Biol.* 324: 871–886.

Nichols, B.J. 2003. GM1-containing lipid rafts are depleted within clathrin-coated pits. *Curr. Biol.* 13:686–690.

Nikonov, A.V., E. Snapp, J. Lippincott-Schwartz, and G. Kreibich. 2002. Active translocon complexes labeled with GFP-Dad1 diffuse slowly as large polysome arrays in the endoplasmic reticulum. *J. Cell Biol.* 158:497–506.

Potter, M.D., and C.V. Nicchitta. 2002. Endoplasmic reticulum-bound ribosomes reside in stable association with the translocon following termination of protein synthesis. *J. Biol. Chem.* 277:23314–23320.

Seiser, R.M., and C.V. Nicchitta. 2000. The fate of membrane-bound ribosomes following termination of protein synthesis. *J. Biol. Chem.* 275:33820–33827.

Wouters, F.S., P.J. Verveer, and P.I. Bastiaens. 2001. Imaging biochemistry inside cells. *Trends Cell Biol.* 11:203–211.